NOTE TO USERS

Model-Based Seizure Detection Method Using Statistically Optimal Null Filters

Liying Shi

A Thesis

in

The Department

of

Electrical and Computer Engineering

Presented in Partial Fulfillment of the Requirements
for the Degree of Master of Applied Science (Electrical Engineering) at
Concordia University
Montreal, Quebec, Canada

March 2005

Your file Votre référence
ISBN: 0-494-04399-7
Our file Notre référence
ISBN: 0-494-04399-7

ABSTRACT

Model-Based Seizure Detection Method Using Statistically Optimal Null Filters

Liying Shi

Long-term EEG monitoring of epileptic patients makes automatic seizure detection necessary, because it is hard for clinicians to interact with the patients or view the recordings continuously.

The problem of seizure detection is inherently difficult because seizure EEG activity consists of a variety of morphologies. It is generally difficult to design a single method that can detect all types of seizures in all patients. In most patients however, one or sometimes two or three types of seizures tend to occur repeatedly. In these cases, the electrographic seizures of each type are similar to each other. Based on this observation, we propose our model –based seizure detection method.

In this thesis, a model-based seizure detection method using *statistically optimal null filters* (SONF) is presented. A template seizure from a patient is first selected, and a set of basis functions that model the template seizure is derived using the proposed modeling methods. Subsequent electroencephalogram (EEG) recording is processed by the SONF and the output represents the noise-free estimate of the seizure. The energy ratio between the output and the input of the SONF is calculated and processed, and used as the test statistic for the seizure detection. Simulation result shows that the modeling Method 4 (Sinusoidal wavelet basis functions) has better performance than other modeling methods. Experiments using 100 hours real SEEG recordings from 5 patients show that the model-based seizure detection method using SONF can lower the false detection rate, and it is most effective for long rhythmic seizures with a clear pattern.

Acknowledgements

I would like to express my deepest gratitude to my thesis supervisors Dr. Rajeev Agarwal and Dr. M. N. S. Swamy, for their continual interest and guidance throughout this work and their generous financial support.

I would like to thank my husband Yunhua for his love and support. I would also like to thank my two sons, David and Kevin, for their patience and being good.

TABLE OF CONTENTS

LIST OF FIGURES

LIST OF TABLES

LIST OF SYMBOLS

AR model	Autoregressive model
ApEn	Approximate Entropy
AWGN	Additive White Gaussian Noise
EEG	Electroencephalogram
IMF	Instantaneous Matched Filter
LTV	Linear Time-Variant
MESWBF	Maximum Energy Sinusoidal Wavelet Basis Functions
MEWBF	Maximum Energy Wavelet Basis Functions
MF	Matched Filter
MMSE	Minimum Mean Square Error
MSE	Mean Square Error
SBF	Sinusoidal Basis Functions
SBR	Seizure to Background Ratio
SEEG	Stereo-electroencephalogram
SNR	Signal to Noise Ratio
SONF	Statistically Optimal Null Filter
SWBF	Sinusoidal Wavelet Basis Functions
WBF	Wavelet Basis Functions
γ'	Energy ratio of the seizure estimate and the observed EEG epoch
γ	Smoothed γ'
δ	The final criterion for the seizure detection

Chapter 1

Introduction

About 80 years ago, Hans Berger succeeded in recording electroencephalogram (EEG)--the electrical activity of the brain. Since then EEG has been used as a non-invasive diagnostic tool in a series of neurological disorders, for example, early diagnosis and localization of brain tumors, coma assessment in intensive care, the definition and assessment of sleep stages, and epilepsy diagnosis. Until today, EEG is still a very important test in neurology clinic, and it is still the leading test used to help diagnose epilepsy.

About 0.5-1% of the population suffer from epilepsy, which is the most common neurological disease next to strokes [1]. Epilepsy is the result of abnormal synchronous discharges in large ensembles of neurons in brain structures. These discharges may be caused by many factors like trauma, tumors, and infections. However, in about half of the patients no specific causative factors are found. The manifestations of epilepsy are bursts of seizures and spikes, which are defined as abnormal EEG patterns. Nowadays, long-term EEG monitoring is used to capture seizures in epilepsy patients, and some automatic seizure detection methods have been developed to solve the problem of detecting seizures in the long EEG recordings.

In this chapter, first we will introduce some basic concepts about EEG and epileptic seizures, and then we will review the existing automatic seizure detection methods. Finally we will give an outline of the thesis.

1.1 What is EEG?

EEG is the electrical activity of the brain. Figure 1.1 is an example of a multiple-channel intracerebral EEG. Nerve cells in the brain are constantly generating very small

electrical signals, whether a person is in wake or sleep state. These small electrical signals are picked up by electrodes placed on the scalp or implanted in the brain, and amplified by the EEG machine so that the signals are observable. Depending on how the electrodes are used, EEG can be specified as either scalp EEG (the electrodes are put on the scalp) or intracerebral EEG (the electrodes are surgically implanted in the brain). Intracerebral EEG is often called stereo-electroencephalogram (SEEG). There are two kinds of EEG recording methods: one is the paper-based analog system, which has been used for over 50 years while the other is the computer-based digital system which is being used more widely during the last 10 years. The availability of the digital EEG allows the application of some advanced analysis tools, such as power spectrum analysis, topographic mapping, source localization, and spike and seizure detection [2].

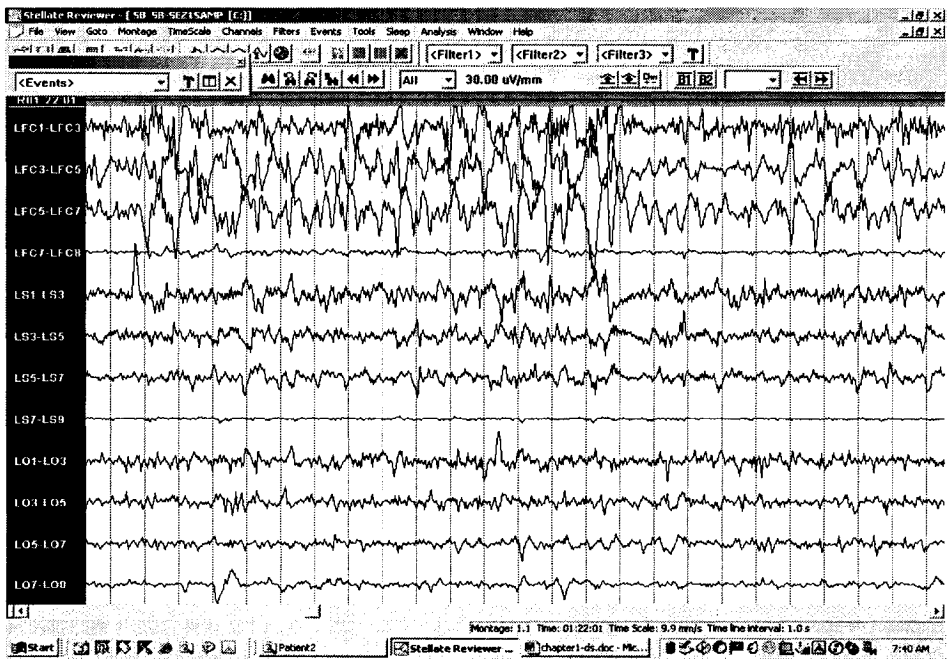

Figure 1.1 Example of background EEG

1.2 What are epileptic seizures?

Epileptic seizures are abnormal, temporary manifestations of dramatically increased neuronal synchrony, either occurring focally (partial seizures) or widespread (generalized seizures) [3]. The cellular and network mechanisms that may contribute to or cause this increased synchrony are still the subject of active investigations. Seizures can be classified into two types, *electrographic seizure* and *behavioral seizure.* An *electrographic seizure* (or *EEG seizure*) is defined as the abnormal paroxysmal EEG pattern, whereas a *behavioral seizure* (or *clinical seizure*) is defined as some clinical manifestations noted by the patient, seen by an observer, or visible on the video, and accompanied by a *electrographic seizure*. Most epileptic seizures are both behavioral and electrographic seizures that can be identified in the review of the video and EEG.

There is no stereotypical pattern that is characteristic of all EEG seizures. Most seizures include some rhythmic discharge of large amplitude. A small-amplitude desynchronized EEG often marks their onset, and at some point during their development, includes activity that is paroxysmal compared to the background. The paroxysm can consist of increased amplitude or increased frequency, activity may likely be rhythmic with frequencies varying in the range of 3 to 29 Hz, and relatively sustained in duration (lasting from several seconds to several minutes). The morphologies of seizures can be of many kinds. Low-amplitude desynchronization, polyspike activity, rhythmic waves at different frequencies and amplitudes, spike and waves can all be seizure activities. Figure 1.2 shows the comparison of background EEG and seizure EEG in several channels.

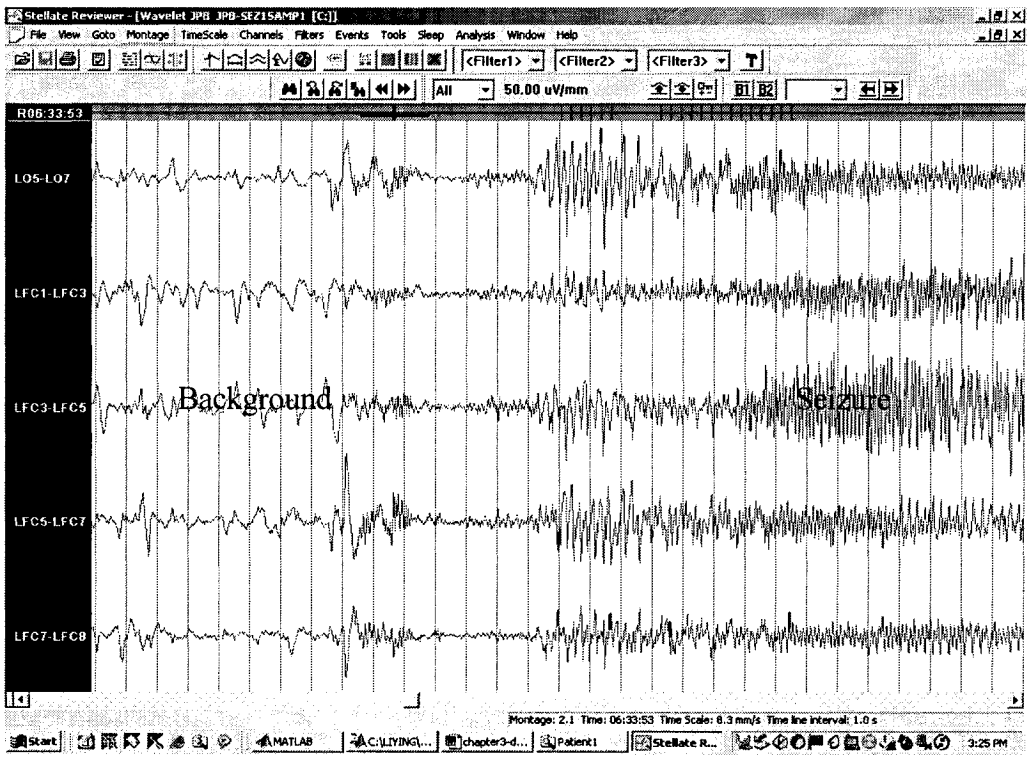

Figure 1.2 Comparison of background EEG and seizure EEG

1.3 How can EEG help in the treatment of seizures and why is automatic seizure detection necessary?

EEG is an important test used to help diagnose and treat epileptic seizures. Many people do not have a detectable brain lesion causing their seizures, and tests like MRI or CT scans show normal brain structure. The EEG, however, can show abnormal electrical function of the brain even when the imaging tests are normal. The long-term EEG consists of the electrical activity of the brain during seizures and non-seizure times. By looking at the patterns of the EEG in different stages the neurologist can identify seizures, the type of epilepsy the patient may have, and what part of the brain is causing the seizures. This information can help the doctor to determine the diagnosis and the type of medication that is appropriate to treat the epilepsy. If medications are not helpful and a

specific brain tissue can be identified as the cause of the seizures, then the patient may be eligible for neurosurgical treatment.

Since the time of a seizure occurrence is not known, in order to capture a number of seizures, it is necessary to establish the long-term EEG and video monitoring system for epileptic patients. Such a system can provide the combined information about the clinical and electrographic seizures, and it is more likely to capture epileptiform abnormalities than a short-term recording. However, it is impossible for the clinicians to continuously observe the EEG or to interact with the patient, since the EEG monitoring sessions can last from several days to weeks [4]. It is a time-consuming and tedious task for the neurologists to review the complete long-term EEG. Moreover, visual review of the vast amount of EEG has the following drawbacks. First, visual inspection lacks standards. Although most neurologists tend to have identical overall conclusions on an EEG data set, they may diverge in the interpretation of specific events [5]. Even the same reader may judge the same event differently at different times. Second, visual inspection lacks quantitative analysis that can uncover hidden character of the data [6, 7]. For these reasons, it is necessary to develop methods for automatic seizure detection.

1.4 Review of automatic seizure detection methods

Automatic seizure detection has been of interest since 1970, but until recently, not many automatic seizure detection methods have been developed. Among the existing methods some function in the time domain, by extracting features such as the amplitude, slope, sharpness (second derivative), and peak-to-peak wave duration. To detect an event, comparisons can be made against fixed thresholds or against the previously observed background EEG patterns. Some other methods are based on neural networks, which

require a large number of sample patterns for training, including the seizure EEG and non-seizure EEG. Wavelet transform and complexity measure have also been used for seizure detection. In the following, we will describe briefly some of these methods.

Gotman [8, 9] presented a method that attempted to recognize a wide variety of seizure patterns. In this method, each EEG channel is broken down into half-waves, which means the original EEG waveform is represented by a seemingly 'sawtooth' signal obtained by connecting adjacent significant extrema of amplitude, and each 'sawtooth' is defined as a half-wave. The EEG recordings are segmented into 2-second epochs and the following features characterize each epoch: the average amplitude of the half-waves relative to that of the background (indicating whether an epoch is paroxysmal), the average duration of the half-waves (indicating frequency), and the coefficient of variation of the half-wave duration (indicating rhythmicity). These parameters are then compared to the predefined thresholds. For a detection to take place, the above parameters must meet some predefined criteria. This method has been integrated to several commercial devices, and it is in relatively widespread clinical use and has been evaluated on large patient groups in diverse clinical environments [10, 11, 12]. The evaluations have indicated that the method detected 70-80% of the seizures, and the false detection rate is one to three false detections per hour. Since an neurologist will later view the EEG recordings, this method is typically set to be overly sensitive in order to capture most of the epileptic seizures at the expense of increased false detections. Improvements to this method have been made to reduce false detections by training the program to "remember" the EEG patterns that caused the false detections for a given patient [13, 14]. In subsequent monitoring, the

program can recognize the same EEG patterns and avoid such false detections. The false detection rate is reduced to 1.26 per hour, but the method becomes more complex.

Harding [15] proposed a seizure detection method to detect seizures in an automated seizure monitoring system. This method detects segments of steep slope in the magnitude of the sample-to-sample differences (MDV) in the signals and counts the number of the large MDVs in the epoch. A large number of steep slopes in an epoch indicate that substantial fast transient activity is present. A segment of steep slope is defined as an MDV when it is larger than a predefined threshold. If the count of large MDVs exceeds the threshold, a seizure has been detected. In 40 monitored patients with a total of 1578 hours of EEG, seizure detection rate was 95%, with an artifact rate of 0.67 per hour.

Murro [16] described a seizure detection method based on discrimimant analysis. First he defined three EEG features-- relative amplitude, dominant frequency and rhythmicity to quantify EEG epochs. The seizure discriminant function D was defined as the logarithm of the relative probability of these quantitative EEG features occurring as seizure or non-seizure EEG:

$$D=\log[P(F1, F2, P1, P2, R1, R2|Sz)/ P(F1, F2, P1, P2, R1, R2|\text{non-Sz})] \quad (1)$$

In (1), (F1, P1, R1) and (F2, P2, R2) are the dominant frequency (F), relative power (P) and rhythmicity (R) of the two channels used to perform detection. P(F1, F2, P1, P2, R1, R2|Sz) and P(F1, F2, P1, P2, R1, R2|non-Sz) are the probabilities of these features occurring as seizure and non-seizure.

Two data sets were used: training data and test data. A test epoch's probabilities of seizure or non-seizure activities are computed using the generalized nearest neighbor method and the training data. A decision is made by comparing the discriminant function D with a threshold. The training data set included 457 seizure EEG epochs from 80 seizures in 18 patients. The test data included 8 patients' seizure and non-seizure EEG. The detection rate ranged from 90% to 100%, and the false detection rate was 1.5-2.5/h.

Another type of seizure detection methods is based on artificial neural network. Webber [17] presented a seizure detection method using a three-layer back propagation artificial neural network. The method can be divided into three stages. First, each channel of the EEG data is divided into adjacent 2 sec epochs of 400 samples. For each epoch, the first stage reduces the 400 data points to 31 context parameters that quantify the amplitude, slope, curvature, rhythmicity, and frequency components of the signal, and these 31 parameters are the input to the second stage. An Artificial Neural Network is the main component of the second stage, and it reduces the 31 parameters to 8 parameters, two of which represent the seizure activity (small seizure, large seizure). The third stage applies simple rules to the output of the second stage and makes a decision as to whether a seizure is present or not. EEG data from 16 patients were used to train the ANN, and EEG data from 50 patients were used to test the method. The detection rate was 76%, with a false detection rate of 1.0/h.

Gabor [18, 19] presented an automated seizure detection method using the self-organizing map (SOM) neural network (NN). The neural network was trained to recognize seizures using 98 training examples. A strategy was devised using wavelet transform to construct a filter that was 'matched' to the frequency features of examples

used to train the NN. Four-second epochs of training examples and EEGs being tested were transformed into time-independent representations of spectrograms resulting in a time-frequency representation of the time-series. Rule-based contextual features were used for detection in association with the NN. This method was evaluated with 200 records from 65 patients (4553.8 h of recording) containing 181 seizures. The result showed that the method detected 92.8% of the seizures with a false detection rate of 1.35 false detections per hour.

Wavelet is a relatively new signal-processing tool. It can provide time-frequency resolution by decomposing the signal in different scales. Khan and Gotman [10] presented an automatic seizure detection method designed for intracerebral EEG (also called stereoelectroencephalogram, SEEG) based on wavelet analysis. This method was aimed at reducing the false detection rate while keeping the sensitivity as high as possible. Daubechies-4 wavelet was used to decompose SEEG into 5 levels. Features (relative amplitude, relative energy, coefficient of variation) were computed for scales 3, 4, and 5 (for a sampling rate of Fs=200Hz, scales 3, 4 and 5 represent the frequency ranges 12.5-25Hz, 6.25-12.5Hz and 3.125-6.25Hz respectively, which cover the seizure frequency range) and compared to the thresholds. If each of the three features passed the corresponding threshold, a preliminary detection was assumed. Extra efforts were made to reduce false detections by 'remembering' the rhythmic bursts occurring commonly in the background. This method was evaluated with 11 patients including 229 hours of SEEG and 66 seizures. The detection rate for this method was 85.6%, and the false detection rate was 0.3/h.

The complexity of the EEG data has led many people to study the EEG as the output of complex systems [2, 20]. Diambra et al. [21] have presented a seizure detection method by computing a complexity measure, the so-called approximate entropy (ApEn), which is a recently developed statistical quantity for quantifying regularity and complexity. This seizure detection method is based on the loss of complexity during the seizure, due to the synchronous discharge of large groups of neurons. A small set data was used to illustrate this method, however its performance was not formally evaluated.

The above is a review of most of the published seizure detection methods since 1980s. It is not an easy task to compare the different seizure detection methods. These difficulties are due to the following reasons. (1) Different methods use different data sets to evaluate the performance of each method. Results are highly dependent on the method of selecting the EEGs on which the evaluation is performed. (2) There is no objective definition of the appearance of a seizure in the EEG. For seizure detection, there are three sets of EEG patterns: those that everyone agrees are seizures, those that are clearly not seizures, and those where opinions differ. It is this last set that makes the comparisons among the various methods difficult, since different EEG readers have significantly different opinions about the last set.

One common thing in the above automatic seizure detection methods is that they all use some general parameterization of seizures, for example, measures such as relative amplitude or frequency are used, rather than some *a priori* information about specific seizures.

Qu and Gotman [4] have proposed a patient-specific seizure *onset* detection method, the first method that uses an existing seizure as template and some non-seizure

background EEG from the patient to detect the *onset* for all the subsequent seizures within the same patient. The main idea of the method is as follows. First, the template is divided into 2.56s overlapping epochs, and the distance between the starting points of two adjacent epochs is 0.32s. For each epoch, five features are extracted: average wave amplitude, average wave duration, coefficient of variation of wave duration in one epoch, dominant frequency, and average power in the main energy zone. These five features from each epoch of the EEG can be considered as a point in the detection space, and the template can then be represented as a set of points in the detection space. By the same procedure, the background EEG can be represented by a set of non-seizure EEG points in the detection space. A classifier of the 'nearest-neighbor' category is trained to classify a new epoch of the EEG into seizure or non-seizure classes. The system was tested using both scalp and intracranial recordings and the detection rate is 100% with a mean detection delay of 9.6 seconds and a false detection rate of 0.21/h.

Compared to the methods described above, this method utilizes some *a priori* information of the patient: a pre-recorded seizure and some background EEG.

1.5 Problem Statement and Outline of the Thesis

The problem of seizure detection is inherently very complex [8, 17], mainly because there is no stereotypical pattern characteristic of all seizures. EEG seizures from scalp recordings are often contaminated by artifacts due to movements and EMG of scalp muscles. Besides, even expert EEG readers can make different conclusions on the same EEG records [6]. Therefore, it is very difficult to design a single method that can detect all types of seizures in all patients.

In most patients, one or sometimes two or three types of seizures tend to occur repeatedly. In these cases, the electrographic seizures of each type are similar to one another (but never identical) [4]. This observation allows us to investigate the idea of model-based seizure detection. That is, if a seizure has previously been detected or visually identified, then it is possible to use this seizure to derive a model for all subsequent detections of the same type of seizures. This strategy is different from the traditional seizure detection methods in that the seizure type to be detected must be *a priori* known in order to build the seizure model. Hence only seizures that belong to the same type as the seizure model will be detected. We have therefore named our proposed method *model-based seizure detection* method.

In our proposed method, the *a priori* known seizure (the *template seizure*) is used to generate a model that describes the intrinsic properties of the seizure to be detected. Estimation of the seizure signal from the subsequent EEG is then performed using the derived model in the context of the *statistical optimal null filters* (SONF). If the observed EEG contains the same type of seizure as described by the model, the output of the SONF will represent the estimate of the seizure. The energy ratio of the output to the input of the SONF is processed and used as the test statistic to decide whether a seizure is present or not.

Comparing our method with that of Qu and Gotman [4], both of the methods require a *priori* known seizure as template. While their method focuses on seizure *onset* detection, our method works on *seizure* detection. From the template seizure, the method of Qu and Gotman extracts some features that define seizure characteristics; however, in contrast, our method extracts some waveforms that model the seizure.

The thesis is organized as follows: Chapter 2 describes the principle of SONFs and summarizes several kinds of SONFs. In Chapter 3, model-based seizure detection method using the SONF and methods of modeling the template seizure are proposed. In Chapter 4, simulated EEG data is first used to test the performance of the six modeling methods, and real SEEG data of five patients are then processed using the best modeling method in the model-based seizure detection method. Chapter 5 contains conclusion and some discussions for future work.

Chapter 2

Statistically Optimal Null Filters

Statistically optimal null filter (SONF) is a novel approach proposed by Agarwal et al. [23, 24] to estimate short-duration signals embedded in noise. It combines a special *instantaneous matched filter* (IMF) that maximizes the signal-to-noise ratio at the output at each instant of time with the least-square optimization criterion. Its intrinsic property is the ability to track signals rapidly, leading to a more practical processing of short-duration signals. It has been shown that the SONF is equivalent to the well-known Kalman filter, but with a much simpler implementation.

In this chapter, *matched filter* and *instantaneous matched filter* (IMF) are briefly introduced, and then several kinds of *statistically optimal null filters* (SONF) based on the IMF are briefly described. Detailed information can be found in [23].

2.1 Instantaneous Matched Filter

A *matched filter* (MF) is a linear filter designed to provide the maximum signal-to noise ratio at its output for a given waveform. Its main application is to detect a known signal from the noisy background. An *instantaneous matched filter* (IMF) is the extension of a *matched filter.*

Consider a known signal $s(t)$ with an *additive white Gaussian noise* (AWGN) *n (t),*

$$x(t) = s(t) + n(t), \qquad t \in [0, T] \tag{2.1}$$

Where $s(t)$ is represented by a single term

$$s(t) = v\phi(t) \tag{2.2}$$

For a given time instant $t = t_1$ in the interval [0, T], the observation interval becomes t_1. As time progresses, the observation interval is continuously increasing to the final

value T. If a *matched filter* (MF) is used to detect the signal $s(t)$ at any given time, then at the output we obtain a signal that provides the maximum output signal to noise ratio, SNR_o, for the considered time interval [0, t_1]. Because the time interval is continually increasing, at each considered time instant, the MF provides a new output signal and a new SNR_o. Hence, it is named as the *instantaneous matched filter* (IMF). The *instantaneous* refers to the current time interval and not to the speed of processing via the MFs. The output of an IMF at time t with $x(t)$ as the input is

$$\upsilon(t) = \int_0^t x(\tau)\phi(\tau)d\tau = vc(t) + n_o'(t) = s_o(t) + n_o'(t) \qquad (2.3)$$

where $n_o'(t)$ represents the output noise, $s_o(t) = vc(t)$ is the output signal that represents the message signal *s(t),* and c(t) is defined as follows,

$$c(t) = \int_0^t \phi^2(\tau)d\tau = \|\phi(t)\|_t^2$$

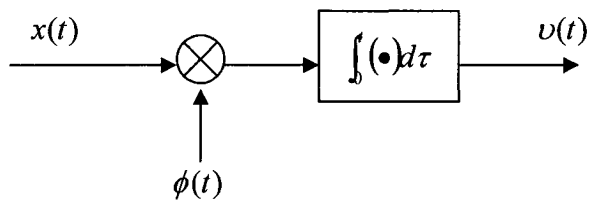

Figure 2.1 Instantaneous Matched Filter

Note that the output $\upsilon(t)$ provides the most reliable (optimal) detection of $s(t)$ at each time t in the presence of zero-mean white Gaussian noise. The only difference is that in the conventional MF, the upper limit of integration is a fixed moment T corresponding to the time at which the detection is made. In our case, the same limit is an independent variable—the instantaneous time. The IMF provides at each instant of time the maximum SNR_o at the output, independent of the amplitude of the signal $s(t)$.

2.2 Statistically Optimal Null Filters

2.2.1 Coherent Null filter

Consider a signal whose waveform shape is known. Let $s(t) = v\phi(t)$, where $\phi(t)$ is known and v is an unknown random variable. Now if we use the IMF, then at time $t_1 \in [0,T]$ the output $\upsilon(t)$ provides the best measure for signal $s(t = t_1)$ to be detected in terms of SNR_o. The notation $s(t = t_1)$ denotes the signal up to time $t_1 \leq T$. From Figure 2.1 and Equation (2.3), we can see that if we now scale $\upsilon(t)$ by $\phi(t)/c(t)$, then the result represents the desired signal $s(t)$ plus some noise,

$$\hat{s}(t) = [vc(t) + n_o'(t)]\frac{\phi(t)}{c(t)} = v\phi(t) + n_o(t) = s(t) + n_o(t) \tag{2.4}$$

Intuitively, $n_o(t)$ becomes smaller and smaller as time grows.

To determine the optimal null filter, the output of IMF $\upsilon(t)$ is scaled by an unknown function $\lambda(t)$ and the result is subtracted from the input to form the output $y(t)$ as shown in Figure 2.2.

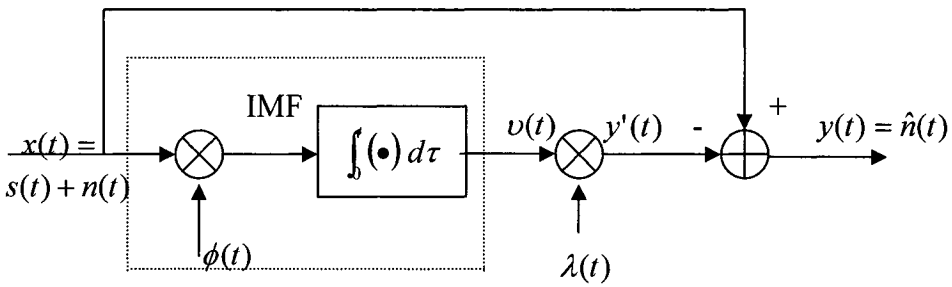

Figure 2.2 Statistically Optimal Null Filter - Coherent Case

$$y(t) = x(t) - y'(t) = x(t) - \hat{s}(t) = \hat{n}(t) \tag{2.5}$$

where the scaled output of the IMF, $y'(t)$, represents the estimate of $s(t)$. Substituting (2.1) and (2.3) in (2.5), $y(t)$ can be written as

$$y(t) = s(t) + n(t) - [vc(t) + n_o'(t)]\lambda(t) \tag{2.6}$$

It now remains to find a suitable function, $\lambda(t)$, such that $y(t)$ represents the input noise $n(t)$ in the minimum mean square error (MMSE) sense. This is equivalent to estimating $s(t)$ with MMSE.

For ideal null filtering, $y_{ideal}(t) = n(t)$, thus the error in filtering becomes

$$e_\lambda(t) = y_{ideal}(t) - y(t) = [vc(t) + n_o'(t)]\lambda(t) - v\phi(t) \tag{2.7}$$

Minimizing the mean-square error, $E[e_\lambda^2(t)]$, with respect to the scaling function $\lambda(t)$, yields

$$\lambda_{opt}(t) = \frac{\phi(t)}{c(t) + 1/SNR} \tag{2.8}$$

where SNR is the input signal-to-noise ratio. Substituting $\lambda_{opt}(t)$ back in (2.7) gives a biased estimate (asymptotically unbiased). Thus, $\lambda_{opt}(t)$ provides statistically optimal but biased null filtering. This is referred to as the *statistically optimal null filter* (SONF).

In order to implement the SONF, knowledge of the input SNR is required. To circumvent this problem, assume that the input noise is weak (i.e., $SNR \to \infty$) then

$$\lambda_{opt}(t) \to \lambda'(t) = \frac{\phi(t)}{c(t)}$$

This is called sub-optimal coherent null filtering.

2.2.2 Non-coherent Null Filter

Consider a case where the signal shape is unknown and $s(t)$ can be written as a linear combination of a set of orthogonal basis functions $\{\phi_i(t), i = 1, 2, \cdots N\}$, as $s(t) = \sum_{i=1}^{N} v_i \phi_i(t)$. Assume that the composing basis functions are *a priori* known while the coefficients v_i's are unknown random variables. For the present, the basis functions are assumed to be orthogonal for any time interval, which is obviously impossible, and this will be addressed later.

Since the coherent null filter is a *linear time-variant* (LTV) filter, the principle of superposition holds. Hence, the non-coherent null filter can be implemented as a set of N parallel branches—one to estimate each term in the expansion of $s(t)$--as shown in Figure 2.3.

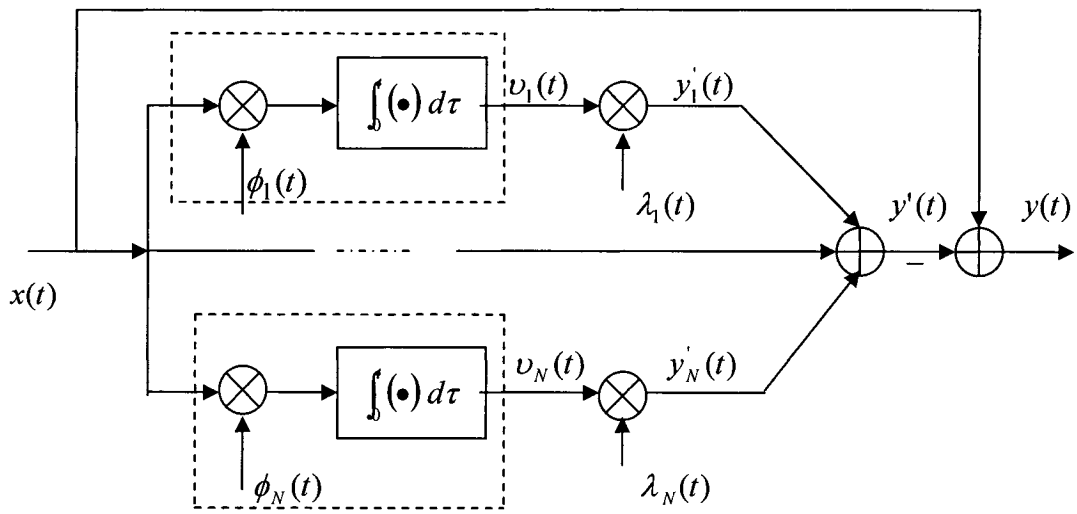

Figure 2.3 Non-coherent Statistically Optimal Null Filters

The basis functions in the expansion of the signal must be orthogonal for any time interval $t \in [0, T]$. One proposed solution is a sliding Gram-Schmidt (GS) orthogonalization of the basis functions at each observation interval as the observation interval increases. This approach is effective, but the computations involved are greatly increased. To avoid this, the assumption of orthogonality of the basis functions is relaxed, which will cause errors in the expected IMF output. It was rationalized in [23, 24] that this error can be minimized by the optimization of $\lambda(t)'s$. Moreover, a globally optimal solution of $\lambda_i(t)'s$ can be obtained where all the $\lambda_i(t)s$ are calculated simultaneously.

2.3 Globally Optimal SONF

To find the $\lambda_{i,opt}(t)$ that are globally optimal, reconsider the problem in vector notation. Referring to Figure 2.3, the followings are defined:

$$\lambda(t) = [\lambda_1(t)\ \lambda_2(t) \cdots \lambda_N(t)]^T$$

$$\upsilon(t) = [\upsilon_1(t)\ \upsilon_2(t) \cdots \upsilon_N(t)]^T$$

$$\phi(t) = [\phi_1(t)\ \phi_2(t) \cdots \phi_N(t)]^T \tag{2.9}$$

$$V = [v_1\ v_2 \cdots v_N]^T$$

where $\lambda(t)$, $\upsilon(t)$, $\phi(t)$ and V are the post IMF scaling functions, outputs of the IMFs, the set of known basis functions and the amplitude of the each term of the desired signal, respectively. By using (2.9), the input signal can be written as

$$x(t) = V^T\phi(t) + n(t) \tag{2.10}$$

And the output signal as

$$y(t) = V^T\phi(t) + n(t) - \lambda^T(t)\upsilon(t) \tag{2.11}$$

The error in suppressing $s(t)$ becomes

$$e(t) = n(t) - \hat{n}(t) = \lambda^T(t)\upsilon(t) - V^T\phi(t) \tag{2.12}$$

and the MSE as a function of $\lambda(t)$ can be written as

$$E[e_\lambda^2(t)] = \eta_\lambda(t) = \lambda^T(t)Q(t)\lambda(t) - \lambda^T(t)\rho(t) - \rho^T(t)\lambda(t) + V^T\phi(t)\phi^T(t)V \tag{2.13}$$

where

$$Q(t) = E[\upsilon(t)\upsilon^T(t)] \tag{2.14}$$

and

$$\rho(t) = E[\upsilon(t)\phi^T(t)V] \tag{2.15}$$

Minimizing (2.15) w.r.t. $\lambda(t)$,

$$\left.\frac{\partial\eta_\lambda(t)}{\partial\lambda(t)}\right|_{\lambda(t)=\lambda_{opt}^g} = 0 = Q(t)\lambda(t) - \rho(t) \tag{2.16}$$

yields the globally optimal solution for $\lambda(t)$

$$\lambda_{opt}^g(t) = [\vartheta D(t) + N_o]^{-1}[\vartheta\phi(t)] \tag{2.17}$$

where the superscript 'g' denotes globally optimal and

$$D(t) = \int \phi(\tau)\phi^T(\tau)d\tau \tag{2.18}$$

and

$$\vartheta = E[VV^T] \tag{2.19}$$

2.4 Discrete Time Recursive Implementation of the Globally Optimal SONF

To implement the exact expressions of the globally optimal post-IMF scaling function $\lambda_{opt}^{g}(t)$, knowledge of the noise and signal power is required, which is usually not possible in practice. To avoid the calculation of $\lambda_{opt}^{g}(t)$, a discrete-time recursive implementation of the globally optimal SONF is presented in [23]. Figure 2.4 outlines the discrete version of the non-coherent case of SONF.

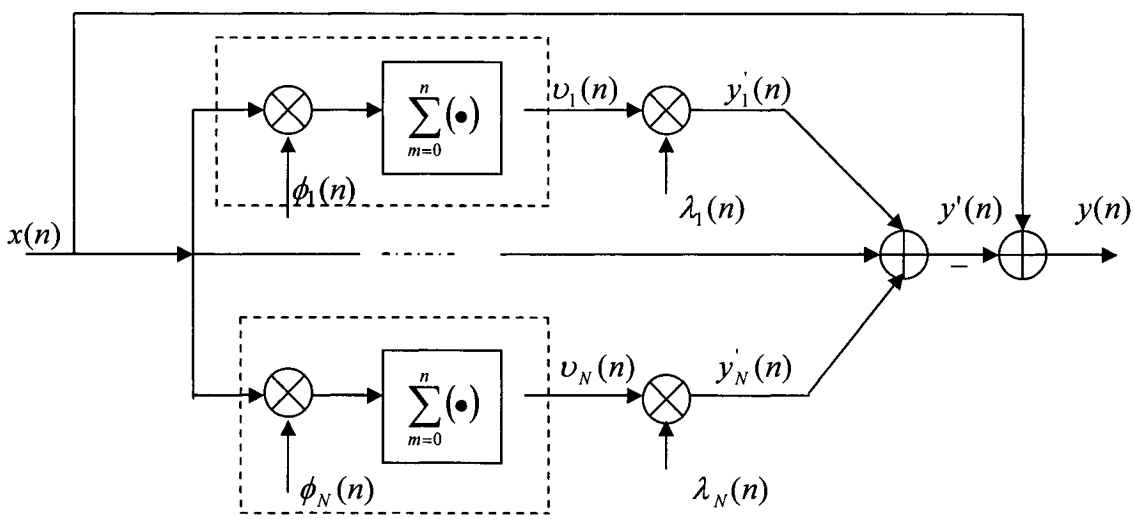

Figure 2.4 Discrete version of the Non-coherent SONF

Equations (2.9) can be written using the discrete variable n as

$$\lambda(n) = [\lambda_1(n)\ \lambda_2(n) \cdots \lambda_N(n)]^T$$

$$\upsilon(n) = [\upsilon_1(n)\ \upsilon_2(n) \cdots \upsilon_N(n)]^T$$

$$\phi(n) = [\phi_1(n)\ \phi_2(n) \cdots \phi_N(n)]^T \tag{2.20}$$

$$V = [v_1\ v_2 \cdots v_N]^T$$

The input $x(n)$ can be written as

$$x(n) = V^T\phi(n) + n(n) \tag{2.21}$$

The output of the IMF is

$$\upsilon(n) = \sum_m^N x(m)\phi(m) = \sum_m^{n-1} x(m)\phi(m) + x(n)\phi(n) = \upsilon(n-1) + x(n)\phi(n) \tag{2.22}$$

and the output $y'(n)$ (the estimate of $s(n)$) can be written as

$$y'(n) = \lambda^T(n)\upsilon(n) = \upsilon^T(n)\lambda(n)$$

The error function

$$e(n) = y(n) - n(n) = \hat{s}(n) - s(n) = \lambda^T(n)\upsilon(n) - V^T\phi(n) \tag{2.23}$$

and the MSE can be written as

$$\eta(n) = E[e_\lambda^2(n)] = E[e_\lambda(n)e_\lambda^T(n)]$$

$$= \lambda^T n)Q(n) - \lambda^T(n)\rho(n) - \rho^T(n)\lambda(n) + V^T\phi(n)\phi^T(n)V \tag{2.24}$$

where

$$Q(n) = E[\upsilon^T(n)\upsilon(n)] \tag{2.25}$$

$$\rho(n) = E[\upsilon(n)\phi^T(n)V] \tag{2.26}$$

Minimizing (2.24) w.r.t. $\lambda(n)$,

$$\left.\frac{\partial\eta(n)}{\partial\lambda(n)}\right|_{\lambda(n)=\lambda_{opt}^g} = 0 = 2Q(n)\lambda(n) - 2\rho(n) \tag{2.27}$$

Assume $D(n)$ is positive definite, we get

$$\lambda_{opt}^{g}(n) = [\vartheta D(n) + N_o]^{-1} \vartheta \phi(n) \tag{2.28}$$

In (2.28)

$$\begin{aligned} \vartheta &= E[VV^T] \\ D(n) &= \sum_{m}^{n} \phi(m)\phi^T(m) = D(n-1) + \phi(n)\phi^T(n) \end{aligned} \tag{2.29}$$

Notice that the original restriction of the orthogonality of the basis functions for any time $t \in [0, T]$ is not used in the development of the globally optimal SONF. Hence, in performing a global optimization of the post-IMF scaling functions, an implicit orthogonalization has been done. Next, the recursive implementation of $\lambda_{opt}^{g}(n)$ is shown to eliminate the need for the knowledge about ϑ and N_o in (2.28).

Let $$R(n) = \vartheta D(n) + N_o \tag{2.30}$$

And $$P(n) = R(n)^{-1} \vartheta \tag{2.31}$$

(2.28) can then be rewritten as

$$\lambda_{opt}^{g}(n) = [\vartheta D(n) + N_o]^{-1} \vartheta \phi(n) = R(n)^{-1} \vartheta \, \phi(n) = P(n)\phi(n) \tag{2.32}$$

Substitute (2.29) into (2.30)

$$\begin{aligned} R(n) &= \vartheta D(n) + N_o = \vartheta D(n-1) + N_o + \vartheta \phi(n)\phi^T(n) \\ &= R(n-1) + \vartheta \phi(n)\phi^T(n) \end{aligned} \tag{2.33}$$

By using (2.31) and (2.33), we can rewrite $P(n)$ as

$$\begin{aligned} P(n) &= [R(n-1) + \vartheta \phi(n)\phi^T(n)]^{-1} \vartheta \\ &= P(n-1) - \frac{P(n-1)\phi(n)\phi^T(n)P(n-1)}{1 + \phi^T(n)P(n-1)\phi(n)} \end{aligned} \tag{2.34}$$

The complete recursive algorithm for implementing the SONF can be written as follows:

$$
\begin{aligned}
&\upsilon(n) = \upsilon(n-1) + x(n)\phi(n) \\
&P(n) = P(n-1) - \frac{P(n-1)\phi(n)\phi^T(n)P(n-1)}{1+\phi^T(n)P(n-1)\phi(n)} \\
&\lambda(n) = P(n)\phi(n) \\
&y'(n) = \upsilon^T(n)\lambda(n)
\end{aligned}
\tag{2.35}
$$

The gain matrix $P(n)$ is initially chosen to be positive definite. As a rule of thumb, one may choose $P(0) = SNR \cdot I$, where I is the identity matrix of order N and $\upsilon(0) = x(0)\phi(0)$.

2.5 Estimation Using Globally Optimal SONF-- An Example

In this section, we use some simulation signals to show the effectiveness of SONFs. There are several kinds of SONFs, here we present some simulations using the globally optimal SONFs in the discrete recursive form. In the next chapter we will use discrete globally optimal SONF to develop our model-based seizure detection methods.

Example: The input $x(n)=s(n)+n(n)$. $s(n)$ is composed of two sinusoids, $s(n) = A * \sin(\omega_0 n + \theta_0) + B * \sin(\omega_1 n + \theta_1)$, and $n(n)$ is an additive white Gaussian noise (AWGN). The signal to noise ratio (SNR) is -5dB. The sinusoidal frequencies ω_0, ω_1 are assumed to be known, and the basis functions used in the SONF are defined as: $\phi_1(n) = \sin(\omega_0 n)$, $\phi_2(n) = \cos(\omega_0 n), \phi_3(n) = \sin(\omega_1 n)$, and $\phi_4(n) = \cos(\omega_1 n)$.

Figure 2.5 shows the estimation of $s(n)$ using globally optimal SONF. Figure 2.6 shows the mean square error (MSE) in estimating $s(n)$. In Figure 2.6, MSE is calculated based on an ensemble average of 500 trials. From the curve, we can see that estimation error mainly exists at the start of filtering. As time goes on, MSE decreases rapidly.

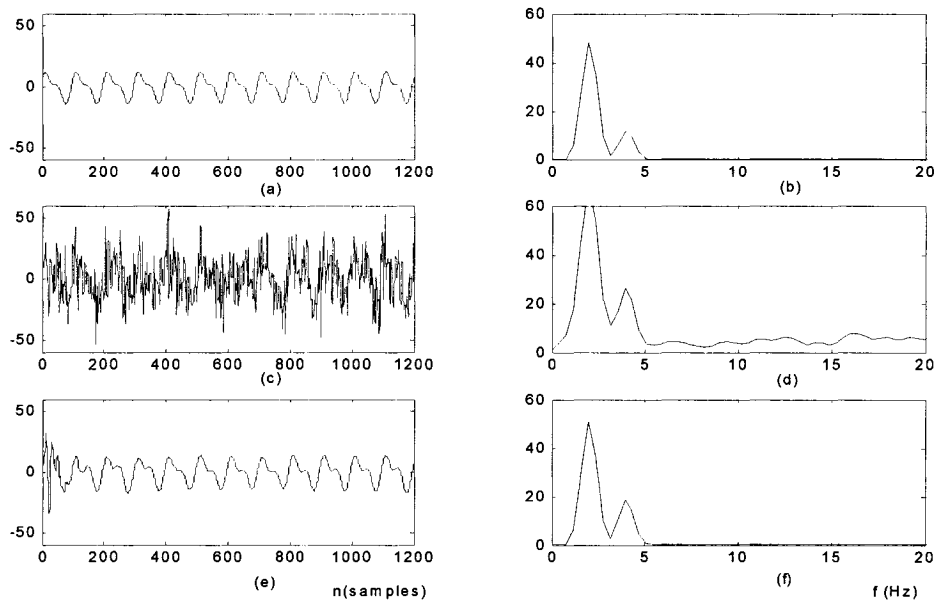

Figure 2.5 Estimation result using globally optimal SONF
(a) Signal $s(n)$; (b) PSD of $s(n)$; (c) mixture $x(n) = s(n) + n(n)$;
(d) PSD of $x(n)$; (e) estimated signal $\hat{s}(n)$; (f) PSD of $\hat{s}(n)$

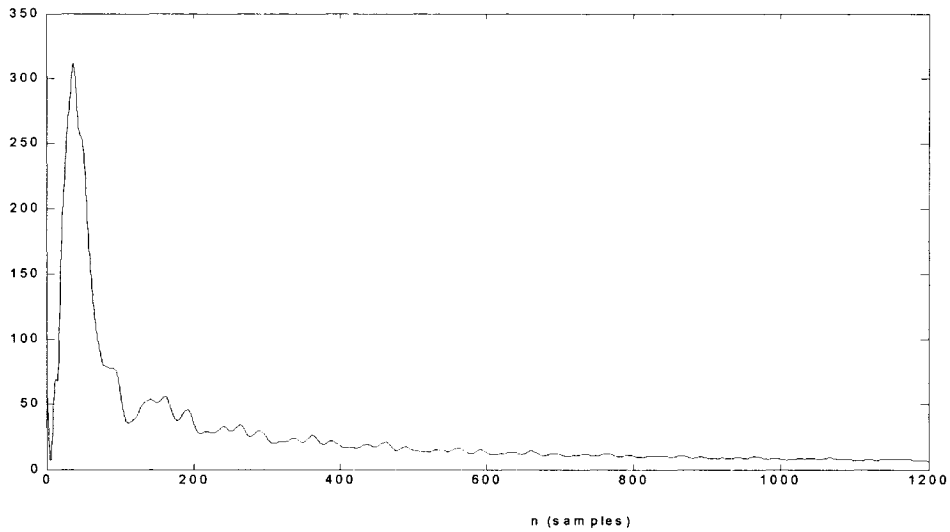

Figure 2.6 MSE in estimating s(n)

Chapter 3

Model-based Seizure Detection Method and Modeling of the Template Seizure

In Chapter 2, we reviewed statistically optimal null filters (SONF) introduced by Agarwal et al. [23, 24]. In this chapter, we propose a model-based seizure detection method using SONF as the basic building block.

3.1 Model-Based Seizure Detection Method

Seizure signal can be considered as a short duration signal compared to the long background EEG. Since our signal of interest is the seizure signal, we may define the detection problem as follows: Let the background EEG (non-seizure activity) represent the noise $n(n)$ and seizure activity as the desired signal $s(n)$. Therefore, the problem can be formulated as the detection of the seizure activity $s(n)$ from the observed EEG that consists of signal plus noise, $x(n) = s(n) + n(n)$.

As mentioned before, in most patients, one or sometimes two or three types of seizures tend to occur repeatedly. In these cases, the EEGs of the same type of seizures tend to be similar to each other, though never identical [4]. For this reason, in our proposed method, the *a priori* known seizure (the *template seizure*) is used to develop a model that describes the intrinsic properties of the type of seizure to be detected. Estimation of the seizure signal from the observed EEG is then performed using the derived model in the context of the SONF. If the observed EEG contains the same type of seizure as described by the model, the output of the SONF will represent the estimate of the seizure. In this case, γ', the energy ratio between the estimated seizure $\hat{s}(n)$ and the observed EEG $x(n)$ is expected to be large. Conversely, if the observation contains only the background EEG $n(n)$, the output should be near zero with little energy; the energy

ratio γ' in this case should be small. Thus, the energy ratio of the estimate of the seizure and the observed EEG can reflect the weight of seizure components in the observed EEG, and it can therefore be used as the test statistic to detect the presence of a seizure in the observed EEG. A large energy ratio value indicates the presence of a seizure, while a small value likely means no seizure. To minimize the spurious peaks, the energy ratio γ' is filtered (moving average) to get a more smooth γ distribution. The final test statistic δ is defined as the difference between the averaged γ value of the test window and that of the background window (the two windows will be defined later). By comparing δ to a threshold, a decision can be made as to whether the input EEG contains a seizure that is similar to the template or not. Figure 3.1 illustrates the general detection scheme [25].

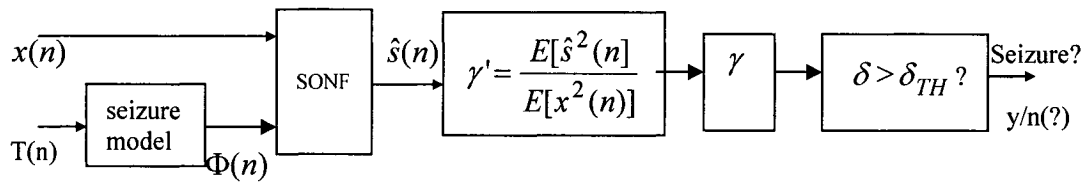

Figure 3.1 Scheme of the model-based seizure detection method

In Figure 3.1, $x(n)$ is the observed EEG, T(n) represents the *template seizure*, $\Phi(n)$ is a set of basis functions derived from the *template seizure* that model the *template seizure* and used by the SONF, γ' the energy ratio of the estimate of the seizure and the observed EEG, γ the smoothed version of γ', δ the final test statistic used to make the seizure detection and δ_{TH} the threshold. The modeling methods will be discussed in Section 3.2.

Globally optimal SONF (discrete time recursive implementation) is used in our model-based seizure detection method to estimate the seizure signal $\hat{s}(n)$ from the observed EEG $x(n)$.

In this initial development of the method, we use a single channel EEG data. EEG data is processed using a sliding window of 6-seconds with a step size of 0.25 seconds, as illustrated in Figure 3.2.

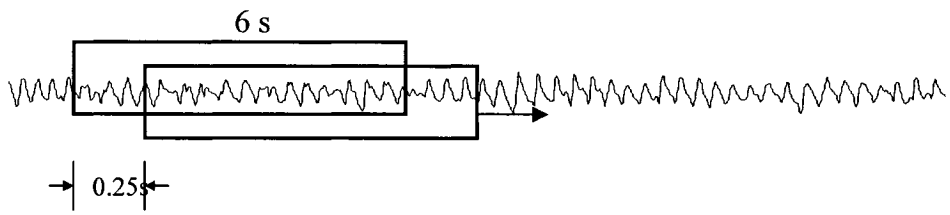

Figure 3.2 Sliding window to process EEG data

The energy ratio (γ') between the estimated seizure and the observed EEG is calculated at 0.25 seconds interval:

$$\gamma' = \frac{\sum_{n=201}^{N} \hat{s}^2(n)}{\sum_{n=201}^{N} x^2(n)}$$

where N=1200, the number of samples in the sliding window given the sampling rate to be 200Hz. The first 200 samples are discarded in the estimation since the estimation error of the SONF is mainly at the start of filtering. As time goes on, the mean square error (MSE) decreases rapidly.

When a seizure is present, large values of γ' will persist for the duration of the template seizure, though not necessarily for each point due to the EEG variations. To

remove spurious peaks in γ', we apply a 24 point moving-average smoothing operation to generate γ. The 24 values of γ' represent a 6-second EEG epoch. The smoothing operation will help in minimizing the spurious peaks during the non-seizure times, while reducing dropouts during seizures.

The final detection criterion δ is defined as the difference between the averaged γ value of the test window and that of the background window. The test window is a 6-second sliding window and the background window is defined as a 30-second sliding window. There is a 30s gap between the two windows, and the purpose of the gap is to prevent the starting part of the seizure from entering the background window. Figure 3.3 illustrates the two windows, and Figure 3.4 shows an example of the distributions of γ', γ and δ.

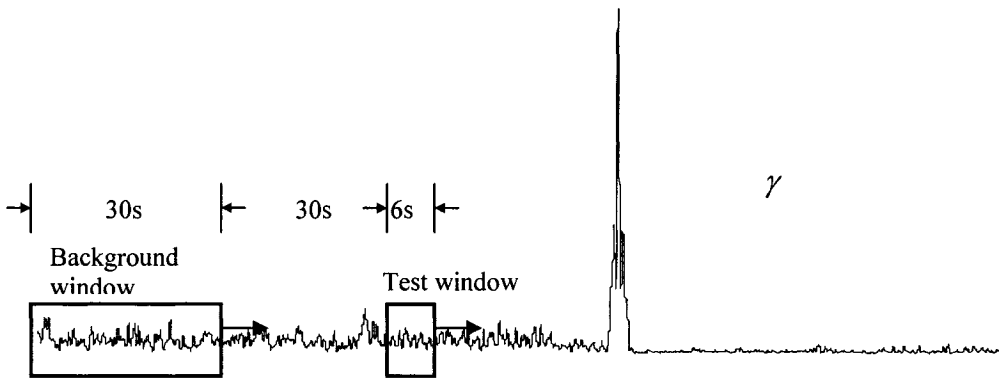

Figure 3.3 Windows used in calculating δ. Background window with duration of 30 seconds. Test window with duration of 6 seconds. There is a 30s gap between the two windows. Both windows slide synchronously.

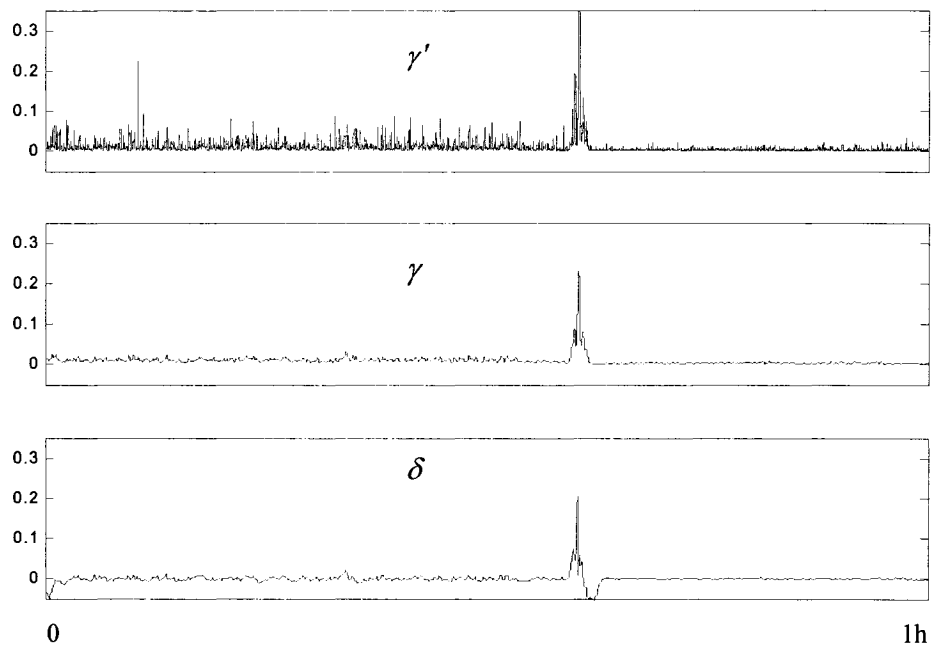

Figure 3.4 Distributions of γ' (top), γ (middle) and δ (bottom))

Seizure can be detected by setting a proper threshold for δ, that is,

if $\delta > \delta_{TH}$, a seizure is detected

if $\delta < \delta_{TH}$, no seizure

Since our model-based seizure detection method performs customized seizure detection for each patient through the *a prioi* known *template*, the threshold δ_{TH} is also determined for each patient. The threshold δ_{TH} is determined as follows: First, the SONF is applied to the *template seizure* and 30 seconds background EEG before the *template seizure*; δ_{TH} is defined as the difference between the averaged γ value of the *template seizure* and that of the 30seconds background EEG.

All detections that occur within 30s of each other are grouped and considered as one seizure activity. For example, if the second detection occurs 15s after the first detection, and the third detection occurs 20s after the second detection, then all three detections are counted as a single detection.

3.2 Modeling of the Template Seizure—Constructing the Basis Functions

In order to use the SONF to estimate/detect seizures, a key step is to construct appropriate basis functions that can model the characteristics of the *template seizure*. Since a seizure can sometimes be as long as several minutes, it is not practical to use the complete seizure as our template. Our purpose is to detect seizure, and the earlier we detect it, the better. Hence, if a seizure is longer than one minute, we take the first minute from the beginning of the seizure as the *template seizure*. In our opinion, this is long enough to represent the important evolving characteristics of the seizure and will not cause missed detections. If a seizure is shorter than one minute, we take the whole seizure as the *template seizure*. Next, according to the length of the *template seizure*, one to three stationary epochs are selected from a single EEG channel by visually inspecting the *template seizure*, and each epoch is chosen to be 6 seconds long for two reasons. First, we want to choose several disjoint stationary epochs to capture the evolving characteristics of the *template seizure*. We expect that three epochs can be sufficient to meet this requirement. Second, 6 seconds is long enough to reflect the main statistical characteristics of the seizure and yet short enough to be relatively stationary. Figure 3.5 is an example of the *template seizure* and the three selected *template epochs.*

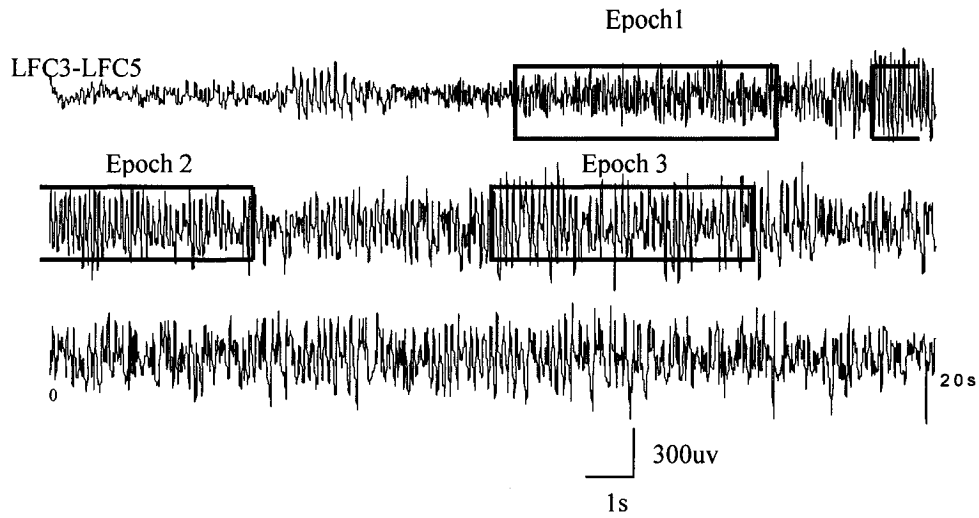

Figure 3.5 Example of a template seizure and the three selected template epochs

These three *template epochs* representing the evolving characteristics of the *template seizure* are used to model the seizure, that is, to construct basis functions required to implement the SONF. We introduce six modeling methods to construct the basis functions. The following describes each of these methods.

3.2.1 Method 1: Direct Method

The most simple and obvious approach is to use the *template epochs* representing the *template seizure* directly as the basis functions. Each of the *template epochs* is normalized and used as a basis function. We use normalization in order to eliminate the influences of the data acquisition and amplification system, since similar seizures at different times may have different amplitudes depending on the recording, environment and of course the physiological condition of the patient. In addition to the normalized template epochs, the Hilbert transforms of the normalized *template epochs* are also used as basis functions. The use of Hilbert transform is necessary since the phase information of the input signal is unknown.

3.2.2 Method 2: Sinusoidal Basis Functions (SBF)

From observation of many seizures, the most intrinsic feature of a seizure is its rhythmic nature. 'Rhythmicity ' is an important common factor of most seizure activities, resulting from the repetitive, self-sustained and synchronized discharges of neurons involved in the epileptic seizures. Compared to the background EEG, seizure activity in some sense can be considered as a deterministic signal. For example, in the time domain, the three *template epochs* in Figure 3.5 clearly show rhythmic nature around some dominant frequencies. Figure 3.6 shows the three *template epochs* and their corresponding power spectra.

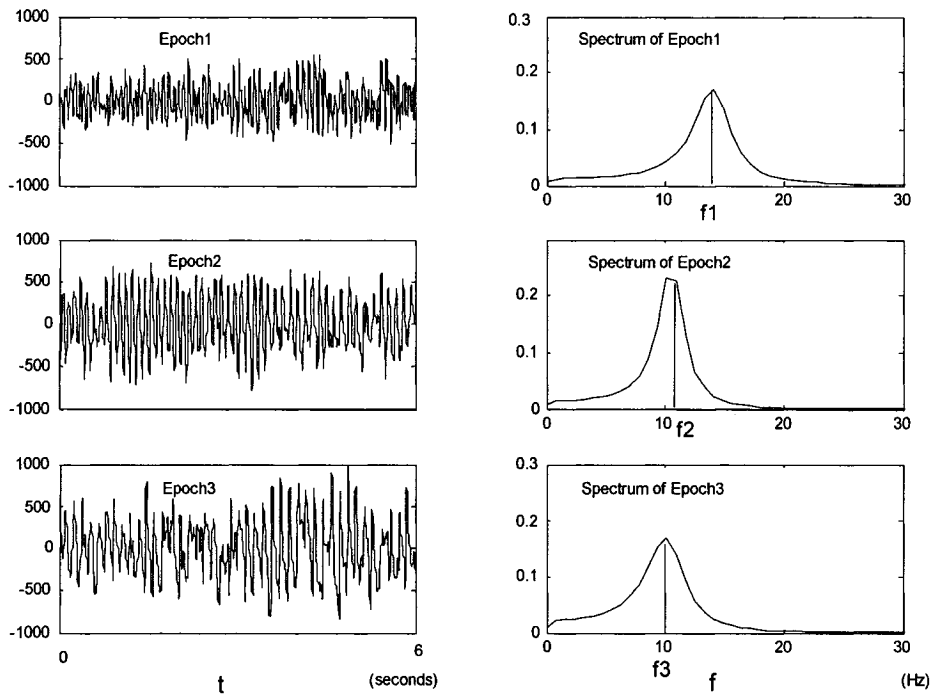

Figure 3.6 Three template epochs and their power spectra

In each spectral graph, a frequency component that is dominant over all the other frequency components can be clearly seen. That is, most of the energy in each *template*

epoch is concentrated at the frequency corresponding to the highest peak value, and this frequency can be considered to be the dominant frequency for each *template epoch*. If f_1, f_2 and f_3 represent the dominant frequencies in each of the three *template epochs* respectively, then the basis functions that can model the seizure can be constructed as sinusoids at these frequencies. Since the knowledge of the phase information of the input signal is unknown, we also use the Hilbert transform of each sinusoid as basis functions. Therefore, six basis functions in all can model the template seizure (for three selected template epochs):

$$\Phi(n) = (\cos\omega_1 n, \cos\omega_2 n, \cos\omega_3 n, \sin\omega_1 n, \sin\omega_2 n, \sin\omega_3 n)$$

3.2.3 Method 3: Wavelet Basis Functions (WBF)

Wavelet transform is an important tool in signal analysis and feature extraction. It has the ability to provide a representation of the signal in both the time and frequency domains. In contrast to the Fourier transform, which provides the description of the overall regularity of signals, the wavelet transform identifies the temporal evolution of various frequencies. This property suits the EEG signal, which is not stationary by its nature, and has a time varying frequency content as well as transient events. This is particularly important for seizures since in most seizures the frequency of the dominant rhythm changes as the seizure evolves.

In order to obtain good results using wavelets, it is important to select a wavelet that matches the shape or the frequency characteristics of the signal at hand. The use of the Daubechies wavelet in the analysis of non-stationary signals such as EEG is well documented. Khan and Gotman [10] used the Daubechies-4 wavelet to detect seizure.

Following their work, we use the Daubechies-4 wavelet to decompose the *template epochs* into different components that can be used to model the *template seizure.*

The Daubechies-4 wavelet is used to decompose each of the *template epochs* into 5 scales of detail components and a residual component. Since the EEG is band-limited to 100 Hz when sampling at 200Hz, the frequency ranges for the five scales are 50-100Hz (scale 1), 25-50Hz (scale 2), 12.5-25Hz (scale 3), 6.25-12.5Hz (scale 4), 3.125-6.25Hz (scale 5). The residual component represents the remaining energy in the range 0-3.125Hz. Figure 3.7 is an example of a *template epoch* and its wavelet decompositions using Daubeties-4 wavelet.

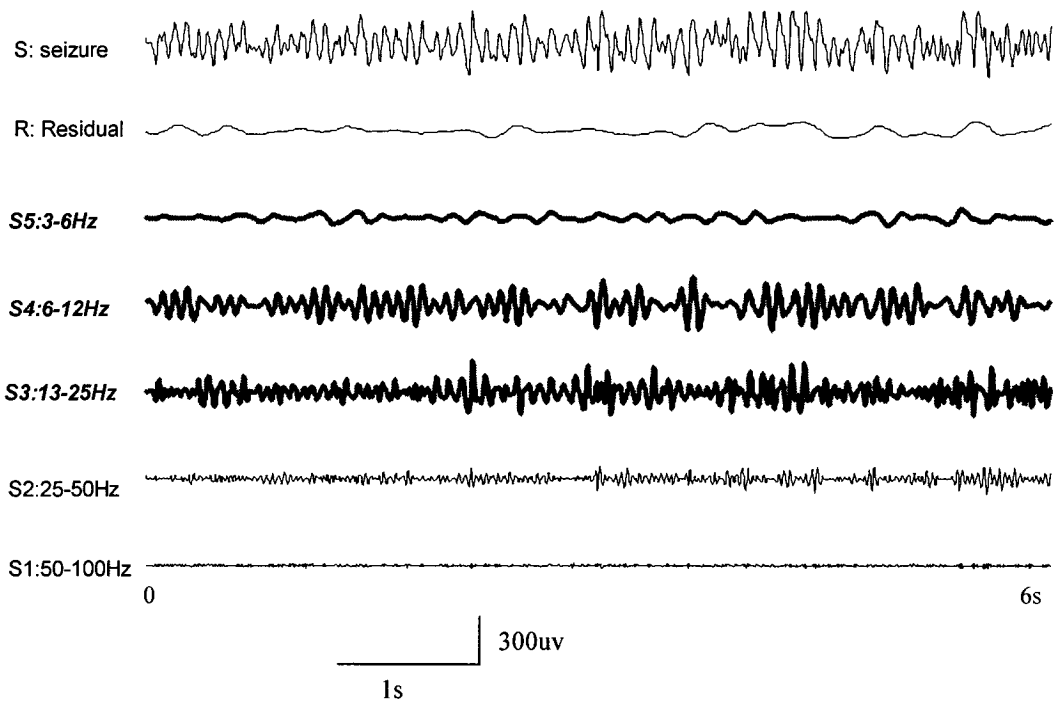

Figure 3.7 Example of one template epoch and its wavelet decompositions. The seizure signal (S) is decomposed into 5 scales and a residual component such that S=S1+S2+S3+S4+S5+R. Scales 3, 4 and 5 cover the seizure frequency range.

Frequency of seizures in intracerebral EEGs is typically in the range of 3-25Hz [10]. For EEG sampled at 200Hz, this is covered by scales 3, 4 and 5. However, the energy distribution in these three scales may vary depending on the seizure under consideration. For instance, some seizures have fairly even energy distributions among scales 3, 4 and 5, while others may have more concentrated energy distributions in one or two of the three scales rather than over all the three scales. In order to highlight the main characters of the seizures and decrease false detections, for each selected template epoch, we select scales from 3, 4 and 5 according to their energy distributions. If the energy of the three scales all exceed 20% of the total energy of the three scales, all the three scales will be selected. If the energy of a scale is less than 20% of the total energy of the three scales, this scale is not considered any further. The selected scale(s) are normalized, and together with its(their) Hilbert transform(s) are used as the basis functions.

3.2.4 Method 4: Sinusoidal Wavelet Basis Functions (SWBF)

In Method 3, we decompose the *template epochs* using wavelet transform and select one to three scales from scales 3, 4 and 5 according to their energy distributions. Since these scales represent seizure activity in a restricted frequency band, clear rhythms are observed. It gives us a new idea of modeling the template seizure where each selected scale in Method 3 is modeled by a sinusoid. The frequency of the sinusoid is the dominant frequency in the power spectrum of that scale. This approach combines Methods 2 and 3, that is, it first separates some noise (like background EEG) and artifacts (like EMG activity) from the *template epochs* by using wavelet transform, and then sinusoids are used to characterize the rhythmicity of the seizure.

3.2.5 Method 5: Maximum Energy Wavelet Basis Functions (MEWBF)

This method is a simplification of Method 3. In method 3, scales are selected to model each *template epoch* according to their energy distributions. In Method 5, for each *template epoch*, only the scale with the largest energy is selected regardless of the energy distributions among the scales 3, 4 and 5. The selected scales from the three *template epochs* are normalized, and together with their Hilbert transforms are used as the basis functions [25]. This method is equivalent to Method 3 when the total energy of the scales 3, 4 and 5 is concentrated in only one of the scales. This method can lower the computational load, but at the expense of losing some of the characteristics of the seizure when the total energy of the scales 3, 4 and 5 is not concentrated in only one of the scales.

3.2.6 Method 6: Maximum Energy Sinusoidal WBF (MESWBF)

This method can be considered as a simplification of Method 4. For each template epoch, after the wavelet transform, the scale with the largest energy among the scales 3, 4 and 5 is modeled as a sinusoid. The sinusoid and its Hilbert transform can be used as basis functions to model each *template epoch*. This method is equivalent to Method 4 when the total energy of the scales 3, 4 and 5 are concentrated in one of the scales. This method can lower the computational load, but at the expense of losing some of the characteristics of the seizure when the total energy of the scales 3, 4 and 5 is not concentrated in one of the scales.

The above six methods can be divided into two classes. The first includes Methods 1, 3 and 5. In this class, each method uses part of the original waveform from the *template seizure* to model the seizure; for example, Method 1 uses the three original *template*

epochs (normalized), and Methods 3 and 5 use part of the original waveforms (Method 3 uses some scales of the wavelet decompositions, and Method 5 uses 1 scale of the wavelet decompositions). The second class includes Methods 2, 4, and 6. In this class, each method extracts some characteristics from the original waveform to model the seizure; for example, all the three methods focus on the seizure's 'rhythmicity'. Method 2 uses one sinusoidal signal to model each *template epoch*, Method 4 uses one sinusoidal signal to model each of the selected scales from scales 3, 4 and 5, and Method 6 uses one sinusoidal signal to model the scale with the largest energy among scales 3, 4 and 5. Table 3.1 summarizes the six modeling methods.

Table 3.1 Summary of the modeling methods

Class 1	Class 2
Method 1: Direct method	Method 2: Sinusoidal Basis Functions (SBF)
Method 3: Wavelet Basis Functions (WBF)	Method 4: Sinusoidal Wavelet Basis Functions (SWBF)
Method 5: Maximum-Energy WBF (MEWBF)	Method 6: Maximum-Energy SWBF (MESWBF)

3.3 Measures Used to Assess the Performance of the Detection Method

In the literature, several measures used to assess the performance of a detection method can be found. These include, for example, missed detections, false detections, true positives, false positives, good detections, false detections, sensitivity, selectivity, detection rate and false detection rate. Many of these terms have identical meaning. The following provides the definitions of the commonly used measures.

- True positives (true detections): the number of seizures identified by the detection method and by the EEG experts.
- False positives (false detections): the number of seizures identified by the detection method, but not identified by the EEG expert.
- Missed detections (false negatives): the number of seizures missed by the detection method, but identified by the EEG experts.
- Sensitivity (detection rate): the ratio of the number of true positives to the total number of seizures identified by the EEG expert.
- Selectivity: the ratio of the number of true positives to the total number of true positives and false positives.
- False detection rate: some people define it as the ratio of the number of false positives to the total number of true positives and false positives. Some people define it as the number of false detections per hour.

In this thesis, we choose two statistical measures to assess the performance of our method, namely, the sensitivity and false detection rate (/hour).

In this chapter, we have developed the model-based seizure detection method using SONF, and have proposed six methods of modeling the template epochs. The criteria and statistical measures that are used in the model-based seizure detection method are also given. In next chapter, we will first use simulated EEG data to test the six modeling methods, and then use SEEG data of five patients to test the *model-based seizure detection method using SONF.*

Chapter 4

Seizure Detection Using Model-Based Seizure Detection Method

In Chapter 3, we proposed a model-based seizure detection method using the SONFs as the basic building block. Several methods of modeling the *template seizure* to construct the basis functions needed for the SONFs were also presented. In this chapter, we present the results of testing the method(s) by using simulated as well as real SEEG data. By using simulated EEG data, we assess the ability of the different methods to model the template seizures, and find out the best amongst these modeling methods. SEEG data from five patients are then processed by our model-based seizure detection method using the best modeling method.

4.1 Simulation

In the first step, we test our methods of modeling the template seizure using simulated EEG data. By using simulations, we try to find as to which among the proposed six methods of modeling the template seizure gives the best result. That is, among the six sets of basis functions generated from the proposed six methods, we select the set that gives the best performance. The performance of a modeling method (or a set of basis functions) is defined as the ability to separate seizure/nonseizure activities. The higher the ability is, the better performance of the modeling method. Later we will define a variable to quantify the performance.

4.1.1 Simulated EEG Data

The simulated EEG is generated using the real SEEG data of one of the patients. The patient's first recorded seizure is used to generate the simulated seizures, and some background EEG data from the same patient are used to generate simulated background EEG.

We use autoregressive (AR) models to generate the simulated signals (both seizure and background EEG). Fourth order AR models are used to generate simulated seizures and 8^{th} order AR models are used to generate simulated background EEG [26, 27].

(1) Simulated seizure EEG

To generate simulated seizures, first we visually select three 6-second disjoint stationary epochs from the patient's real seizure signal. This is the same process as choosing the *template epochs* from the *template seizure*. These three epochs represent the characteristics of the seizure at three different times during the seizure.

Each selected epoch is modeled with a 4^{th} order AR model [26, 27]. Thus, three AR models will be constructed from the three *template epochs*. Zero-mean AWGN is used to excite each of the three AR models, and the output of each AR model is 10 seconds in duration. The three outputs are concatenated to form the simulated seizure that is 30 seconds in duration. By using this method, 37 simulated seizures are generated. The first simulated seizure is used as the *template seizure* to derive the basis functions using each of the modeling method; the other 36 seizures are used to test the performance of the six modeling methods. Figure 4.1 shows an example of the three *template epochs* of a real seizure and the corresponding three epochs of the simulated seizure generated using the above procedure.

Since all the 37 seizures are generated from the same three AR models, their statistical characteristics are the same, and therefore they can be considered to belong to the same type of seizure.

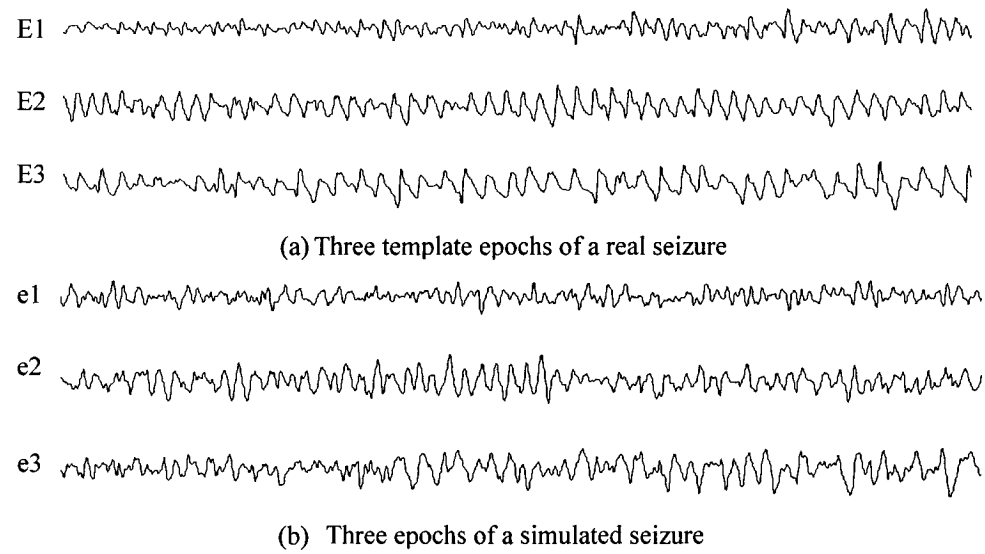

Figure 4.1 Example of a real seizure and a simulated seizure (a) three template epochs of a real seizure (b) three epochs of a simulated seizure

(2) Simulated background EEG

The main idea in generating simulated background EEG is similar to that used for generating simulated seizure EEG. First, twelve segments of background EEG are selected from the patient's EEG recordings. Since these segments are selected at different times during the recording, they are expected to represent different background EEG patterns, and each segment is 6 seconds long. Each selected segment is modeled with an 8^{th} order AR model [26, 27]. In total, 12 AR models are constructed, one for each of the 12 background EEG segments.

Zero-mean additive white Gaussian noises are then used to excite each of the 12 AR models. The output of each AR model is 5 minutes long. Hence, we will get 12 pieces of simulated background EEG with duration of 5 minutes each. Figure 4.2 shows an example of a real background EEG and its simulated background EEG.

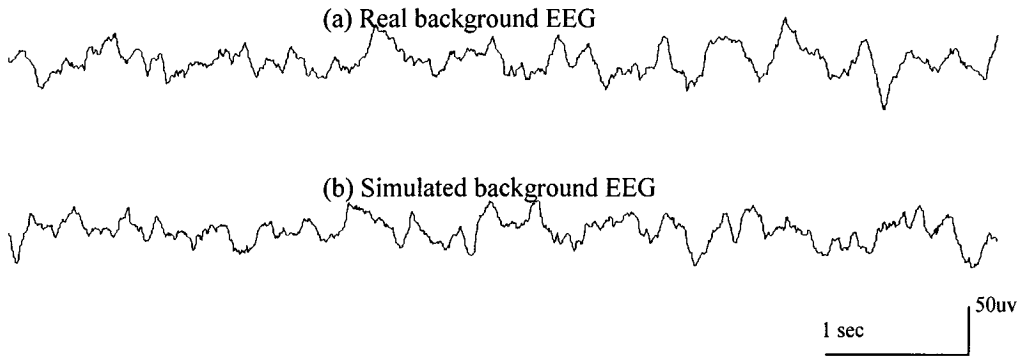

Figure 4.2 Example of real background EEG and simulated background EEG (a): real background EEG. (b): simulated background EEG.

(3) **Simulated EEG data**

As mentioned earlier, we have generated 37 simulated seizures, each of 30-second duration and 12 pieces of simulated background EEG, each of 5-minute duration. The first simulated seizure is used as the *template seizure* to generate the basis functions needed in the *model-based seizure detection method* using SONF. The remaining 36 simulated seizures are then combined with the 12 pieces of simulated background EEG. For each segment of the 5-minute simulated background EEG, three simulated seizures are superimposed at different times.

During a seizure, the contribution of the seizure to the total EEG activity is generally much higher than the background EEG, resulting in a relatively high *seizure-to-background ratio* (SBR),

$$SBR = 10\log_{10}\frac{E(sez^2)}{E(bg^2)}$$

In the above equation, $E(sez^2)$ represents the seizure energy and $E(bg^2)$ represent the energy of the background EEG. Hence, seizure and background EEG are not simply added together. The simulated background EEG during the seizure times is scaled down to satisfy the desired SBR value. In our simulation, we use SBR=20dB [28].

To simulate the real situation, a measurement noise assumed to be AWGN is added to form the final observed simulated EEG data. The level of noise is controlled by the desired *signal-to-noise ratio* (SNR)

$$SNR = 10\log_{10}\frac{\sigma_s^2}{\sigma_n^2}$$

where σ_n^2 is the variance of the measurement noise, and σ_s^2 is the energy of the simulated EEG.

4.1.2 Performance Comparison of Different Basis Functions Using Simulated EEG Data

As mentioned earlier, the first simulated seizure is used as the *template seizure* to construct the basis functions using each of the modeling method; the other 36 seizures are used to test the performance of the six modeling methods.

(1) Constructing the Basis Functions

The basis functions are constructed from the *template seizure* using the six modeling methods proposed in Chapter 3. Figure 4.3 shows the *template seizure* (the first simulated seizure) and the three selected *template epochs* (Epoch1, Epoch2 and Epoch3, each of 6 seconds each).

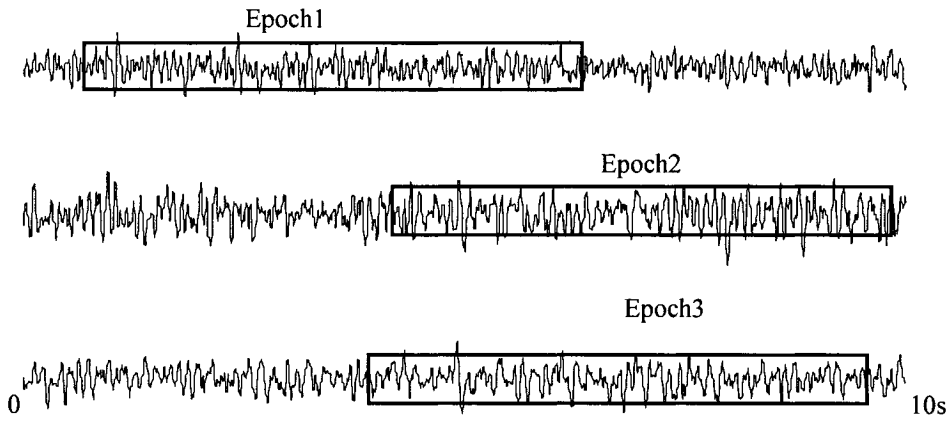

Figure 4.3 The template seizure (the first simulated seizure) and the template epochs

I. Constructing the basis functions using Method 1 (Direct method)

As the first step, the template epochs Epoch1, Epoch2 and Epoch3 are normalized by L_2-norm, i.e.

$$X_i = \frac{\widetilde{X}_i}{\|\widetilde{X}_i\|}, \qquad i=1, 2, 3$$

where $\widetilde{X}_i$ (i=1, 2, 3) represent the *template epochs* and X_i are the normalized epochs. Hilbert transform is then applied to the normalized vectors to get *Y*1, *Y*2 *and Y*3.

The normalized *template epochs* and their corresponding Hilbert Transforms form the set of basis functions corresponding to Method 1.

$$\Phi_1(n) = (X1, X2, X3, Y1, Y2, Y3).$$

II. Constructing the basis functions using Method 2 (SBF)

Consider a system driven by white noise. The current output *s(n)* of the system relies on the previous outputs *s(n-k)* and the current input *w(n)*, $s(n) = w(n) - \sum_{k=1}^{p} a_k s(n-k)$. The transfer function of the system is

$$H(z) = \frac{1}{1 + \sum_{k=1}^{p} a_k z^{-k}}$$

This system is called a *p*-th order AR model. If the variance of the white noise σ_w^2 and the AR parameters a_i are known, the power spectrum density of *s*(n) can be calculated using the following equation

$$S_s(e^{j\omega}) = \left|H(e^{j\omega})\right|^2 \sigma_w^2$$

We use 2nd order AR models to estimate the power spectra of the three *template epochs*. Burg method is used to estimate the coefficients of the AR models and the variance of the white noise. Dominant frequency of each *template epoch* is determined by finding the frequency corresponding to the peak value of each spectrum. Figure 4.4 shows the power spectrum of Epoch1.

In Figure 4.4, the frequency f_1 corresponds to the peak value of the power spectrum, and it is considered as the dominant frequency in Epoch1. By the same procedure, the dominant frequencies of Epoch2 and Epoch3 are found.

If f_1, f_2, f_3 are the dominant frequencies of the three template epochs, the set of basis functions corresponding to modeling Method 2 can be expressed as a set of sinusoidal signals at these frequencies,

$$\Phi_2(n) = (\sin 2\pi f_1 n, \sin 2\pi f_2 n, \sin 2\pi f_3 n, \cos 2\pi f_1 n, \cos 2\pi f_2 n, \cos 2\pi f_3 n).$$

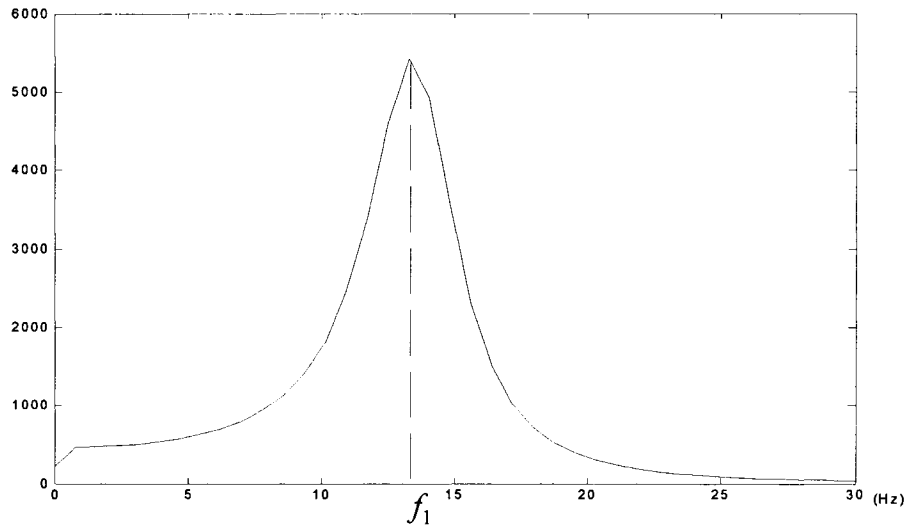

Figure 4.4 The power spectrum of Epoch1

III. Constructing the basis functions using Method 3 (WBF)

The Wavelet transform of a signal $x(t)$ is defined as

$$WT_x(a,\tau) = \frac{1}{\sqrt{a}} \int_{-\infty}^{\infty} x(t)\psi^*(\frac{t-\tau}{a})dt, \qquad a \geq 0 \qquad (4.1)$$

In (4.1), $\psi(t)$ is called mother wavelet, and $\psi(\frac{t-\tau}{a})$ is the shifted and scaled version of $\psi(t)$. a is the scale parameter, τ is the shift parameter.

The Daubechies-4 wavelet is used to decompose each of the *template epochs* (Epoch1, Epoch2 and Epoch3) into 5 scales of detail components and a residual component. We use the discrete wavelet transform in our method. Figure 4.5 shows the decomposition of Epoch1.

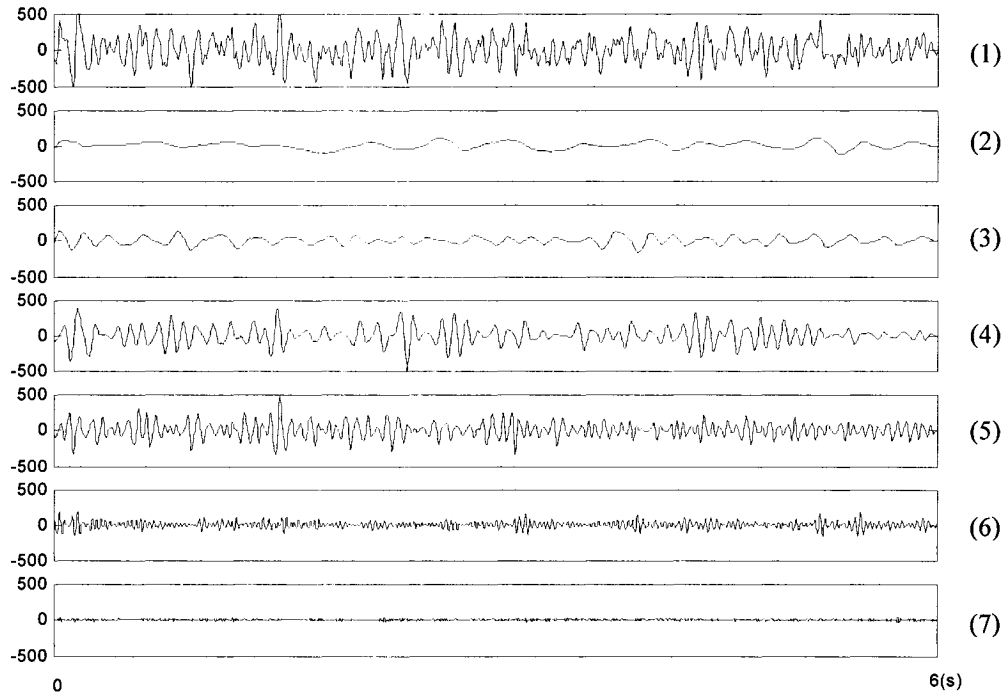

Figure 4.5 The wavelet decomposition of Epoch1. (1) Epoch1, (2) residual signal, (3)-(7): scale 5 – scale 1.

As mentioned earlier, scales 3, 4 and 5 cover the seizure's frequency range. Percentages of energy distributions among the three scales for each *template epoch* are then calculated. For Epoch1 in our example, the energy distribution among the three scales is: 43.24% (scale 3), 43.22% (scale 4), and 13.54% (scale 5). For Epoch2, they are 25.43%, 58.35% and 16.22%, and for Epoch3, 19.27%, 54.87% and 25.86%.

The scales with the energy percentage greater than 20% are selected from the three *template epochs*. Therefore, scales 3 and 4 from Epoch1, scales 3 and 4 from Epoch2, and scales 4 and 5 from Epoch3 are selected. These selected scales are then normalized (L_2-norm), and together with their Hilbert Transforms form the WBF.

IV. Constructing the basis functions using Method 4 (SWBF)

The SWBF corresponding to Method 4 are constructed as follows. Each selected scale in Method 3 is modeled by a sinusoid. The frequency of the sinusoid is the dominant frequency of the power spectrum of that scale, which is estimated using a 2nd order AR model as described in Method 2. The sinusoids and their Hilbert Transforms compose the SWBF.

V. Constructing the basis functions using Method 5 (MEWBF)

To construct the basis functions using Method 5, first the wavelet decomposition is performed as described in Method 3. After wavelet decomposition, for each *template epoch*, only the scale with the largest energy is selected from scales 3, 4 and 5. Hence, scale 3 from Epoch1, scale 4 from Epoch2, scale 4 from Epoch3 are selected. Each of these selected scales are then normalized and together with their Hilbert Transforms, they form the MEWBF.

VI. Constructing the basis functions using Method 6 (MESWBF)

To construct the basis functions using Method 6 (MESWBF), the selected scales in Method 5 are modeled by sinusoids. Frequencies of the sinusoids are dominant frequencies of the power spectra of these scales. The sinusoids and their Hilbert Transforms compose the MESWBF.

In the above, we have introduced the implementation of the six sets of basis functions using the six modeling methods. Next we compare the performance of the six sets of basis functions using the simulated data.

(2) Performance Comparison

The model-based seizure detection method is then applied to the simulated EEG data using the six sets of basis functions generated from the *template seizure*. As stated in Chapter 3, the energy ratio (γ') between the seizure estimate and the observed EEG is first calculated and a 24-point moving average is then applied to γ' to get γ. Figures 4.6-4.11 show examples of γ' and γ distributions of the six modeling methods using the simulated data. In these figures, SNR=20dB, and SBR=20dB.

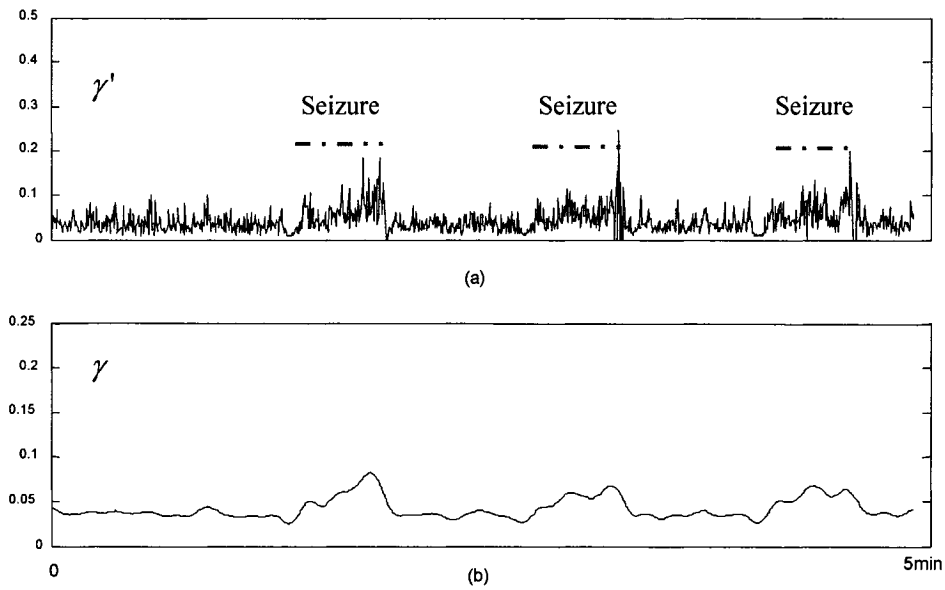

Figure 4.6 Distributions of γ' and γ using modeling Method 1-Direct method. (a) γ' (b) γ. The dash-dot lines indicate the seizure locations.

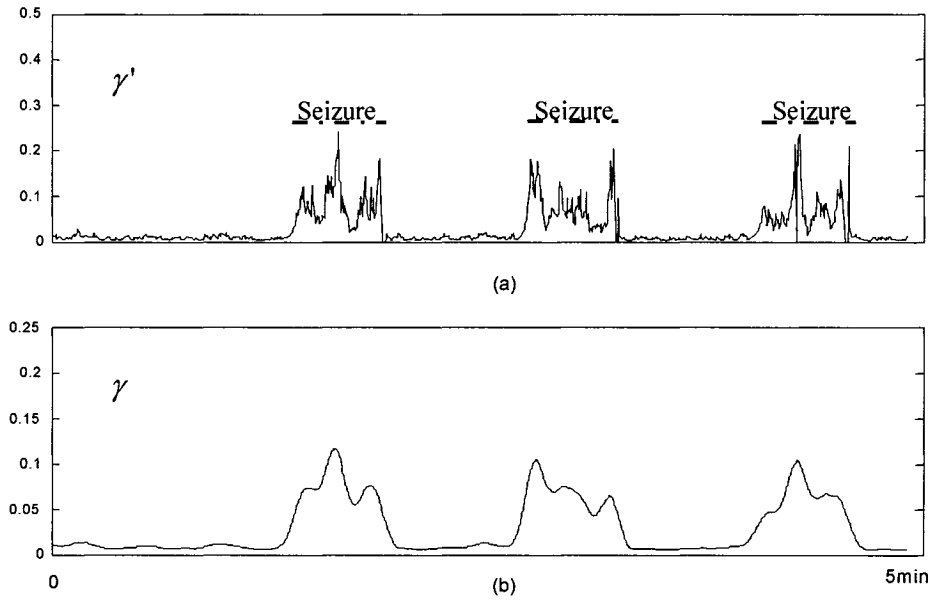

Figure 4.7 Distributions of γ' and γ using modeling Method 2-Sinusoidal Basis Functions (SBF). (a) γ' (b) γ. The dash-dot lines indicate the seizure locations.

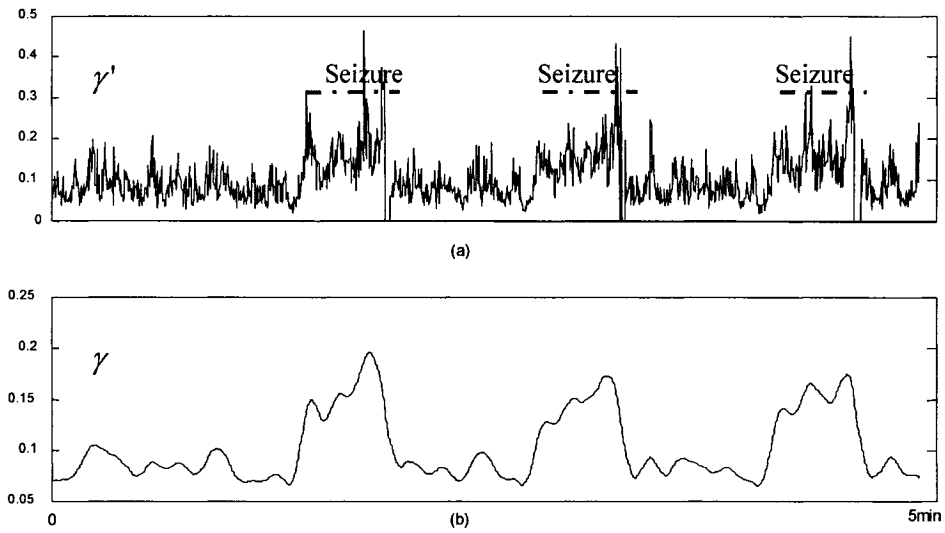

Figure 4.8 Distributions of γ' and γ using Method 3- Wavelet Basis Functions (WBF). (a) γ' (b) γ. The dash-dot lines indicate the seizure locations.

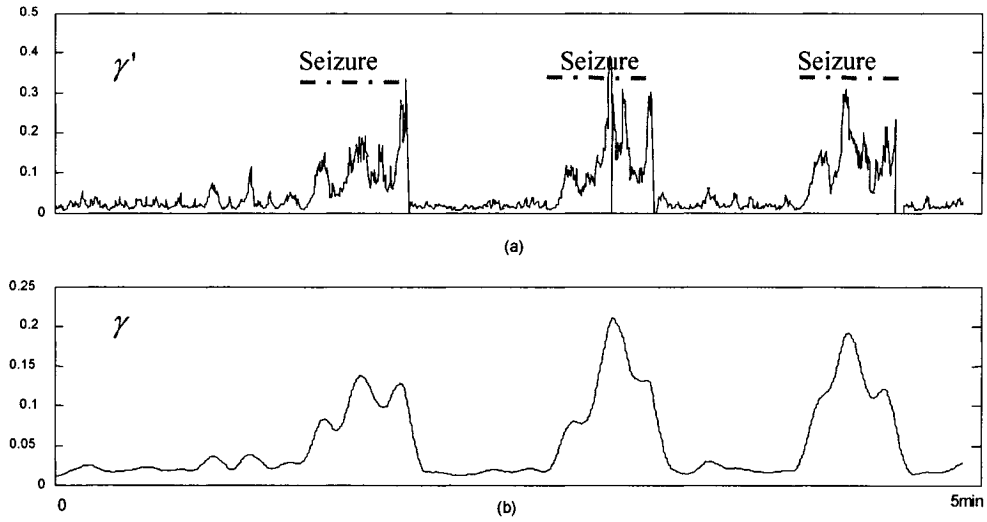

Figure 4.9 Distributions of γ' and γ using modeling Method 4- SWBF. (a) γ' (b) γ. The dash-dot lines indicate the seizure locations.

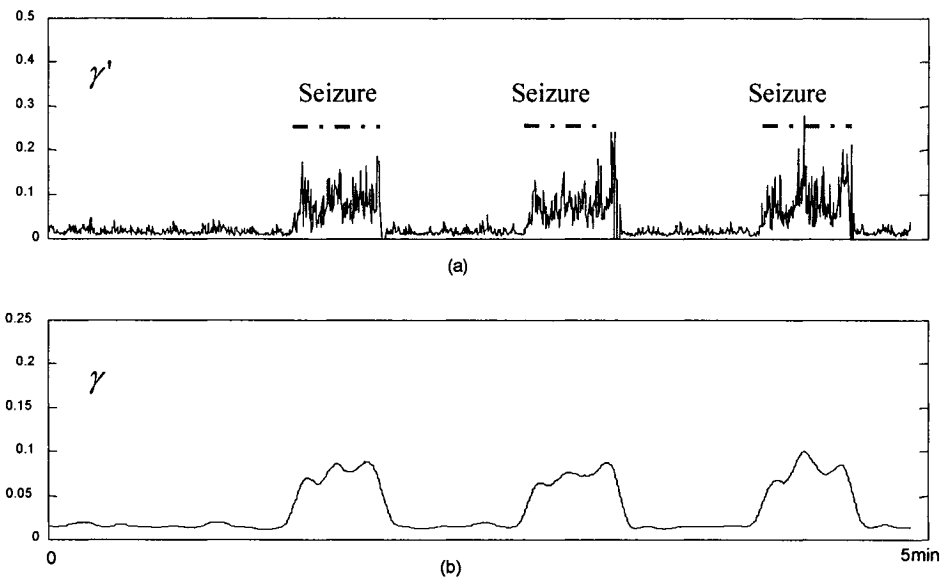

Figure 4.10 Distributions of γ' and γ using modeling Method 5- MEWBF. (a) γ'; (b) γ. The dash-dot lines indicate the seizure locations.

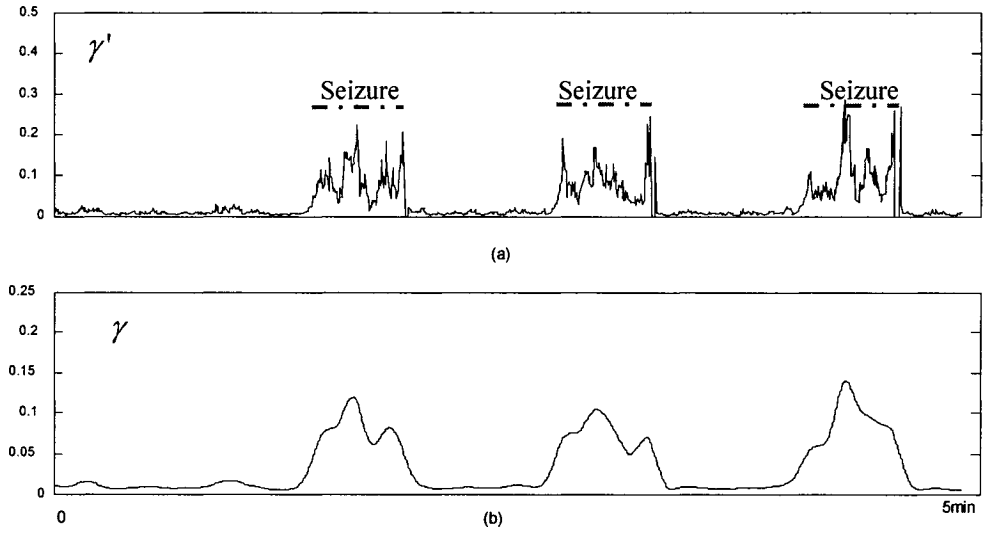

Figure 4.11 Distributions of γ' and γ using modeling Method 6- MESWBF. (a) γ' (b) γ. The dash-dot lines indicate the seizure locations.

From these figures, we can see that after applying the smoothing operation on γ', except for Method 1 (Direct Method), all the γ distributions show prominent peaks at the seizure locations. In order to compare the performance of the six sets of basis functions, we apply the model-based seizure detection method to the simulated EEG data at different SNR levels (SNR= -10, -5, 0, 5, 10, 15, 20dB) using the proposed six sets of basis functions.

We use $\Delta\gamma$ to assess the performance of the basis functions (the ability to separate seizure/nonseizure activities), where $\Delta\gamma$ is defined as the difference between the average γ value during the seizure ($\bar{\gamma}_{sez}$) and the average γ value of the 30 seconds during non

seizure times before the seizure ($\bar{\gamma}_{bg}$), that is $\Delta\gamma = \bar{\gamma}_{sez} - \bar{\gamma}_{bg}$. Figure 4.12 illustrates this process. The greater the value of $\Delta\gamma$ is, the better the performance of the set of basis functions.

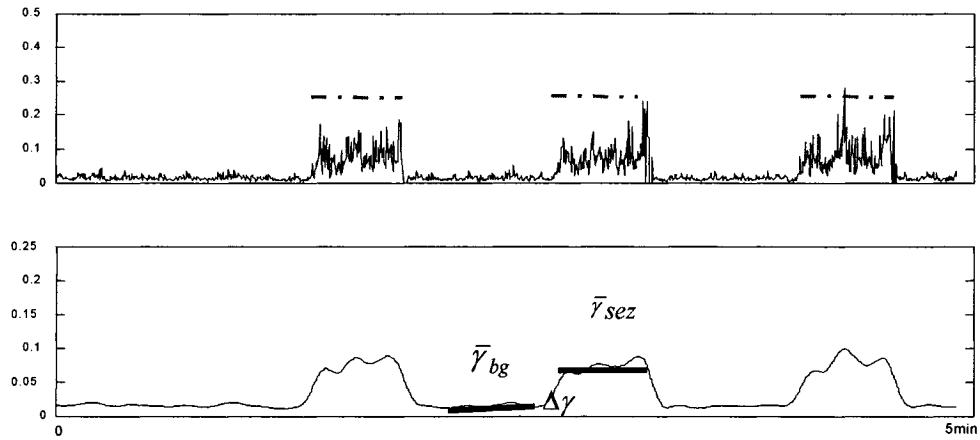

Figure 4.12 Illustration of $\bar{\gamma}_{sez}$ and $\bar{\gamma}_{bg}$. $\bar{\gamma}_{sez}$ is the average γ value during the seizure, $\bar{\gamma}_{bg}$ is the average γ value of the 30 seconds during non seizure times before the seizure. $\Delta\gamma = \bar{\gamma}_{sez} - \bar{\gamma}_{bg}$.

For each fixed SNR level, the performance of each set of basis functions is evaluated based on the mean $\Delta\gamma$ values from the 36 simulated seizures. The mean values and standard deviations of $\Delta\gamma$ from the six sets of basis functions are presented in Figure 4.13. For convenience of comparison, the mean values of $\Delta\gamma$ associated with the six sets of basis functions are also depicted in Figure 4.14.

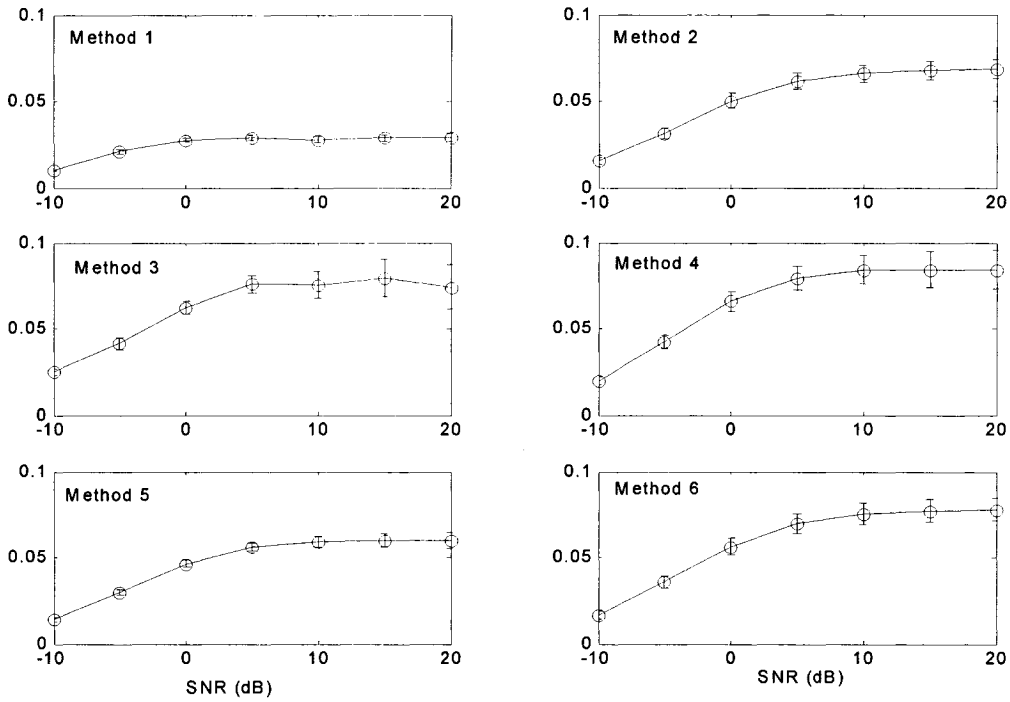

Figure 4.13 Mean values and standard deviations of $\Delta\gamma$ from the six sets of basis functions

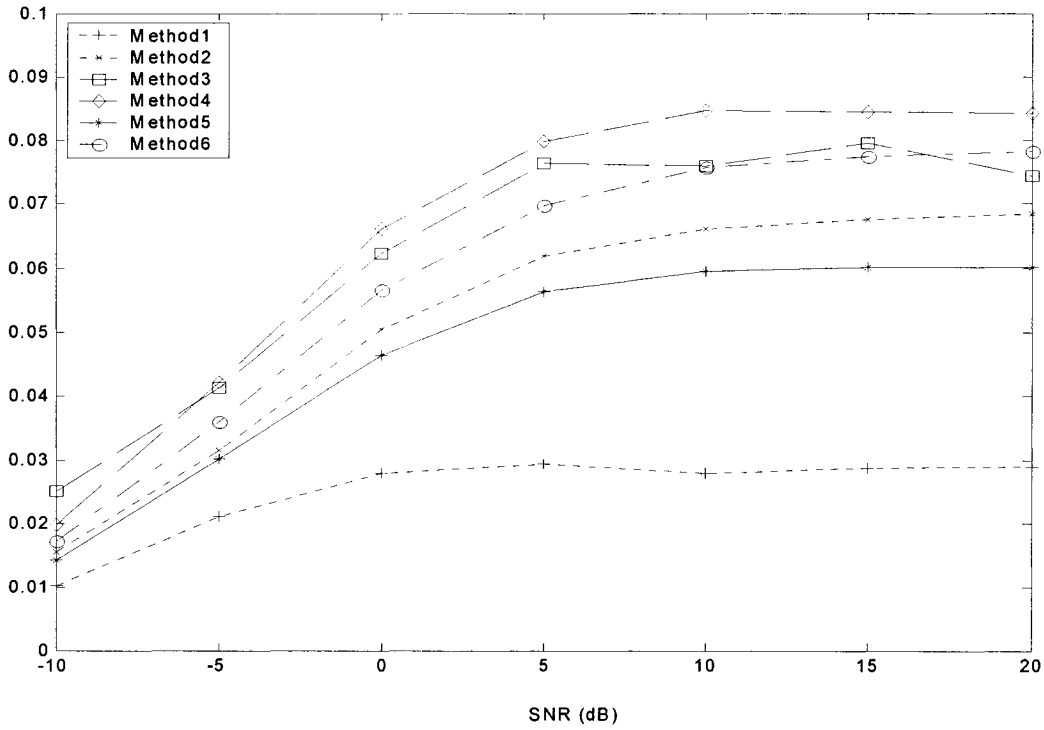

Figure 4.14 Performance comparison of the six sets of basis functions

From these two figures, we can see that as the SNR decreases below 5dB, the $\Delta\gamma$ values of all the basis functions show a monotonic decease; however, when the SNR increases beyond 5 dB, the $\Delta\gamma$ values do not increase appreciably. That is, the values are stabilized.

Among the six sets of basis functions, the basis functions generated by Method 1 (Direct method) shows the worst performance. The $\Delta\gamma$ curve is far lower than those of the other five methods at all SNR levels. Basis functions generated by Method 4 (SWBF) show the best performance. The $\Delta\gamma$ values for Method 4 are greater than that of all the other methods at almost all the tested SNR levels.

In the following, we will apply our model-based seizure detection method to some real SEEG data using the basis functions generated by Method 4 (SWBF).

4.2 Real SEEG Data

The simulation results in the previous section show that the set of basis functions generated by the proposed modeling Method 4 (SWBF) provided the best performance. In this part, real stereo-electroencephalogram (SEEG) data of five patients are processed to evaluate the model-based seizure detection method using the SONF and the modeling Method 4 (SWBF).

4.2.1 Subjects

In order to evaluate a detection method, one important factor is the selection of the data. The data should in no way be pre-selected [29] to address specific cases. That is, the performance of any method can be highly dependent on the data set used for the development. By pre-selecting the data set, it is possible to achieve a very high detection rate and a very low false detection rate, but in fact the method may not be robust and may not perform so well on a different data set. Hence, we randomly select five patients as our test subjects. All the patients had intracerebral recordings sampled at 200Hz and the SEEG data was stored on CDs. Each patient had five recordings including three recordings with seizures, one without seizures when the patient was awake, and one without seizures when the patient was asleep. Each recording was about 4 hours long (sometimes 5 hours long). In all, each patient had about 20 hours SEEG data containing at least three seizures. More information about each patient's recordings is given in Tables 4.1-4.5. For each patient, only one channel data was used. The EEG channel was selected as the one in which the seizure was most prominent as identified by the reviewer.

Table 4.1: Patient JPB (selected channel: LH1-LH3)

Files	JPB-SEZ1	JPB-SEZ2	JPB-SEZ3	JPB-Sleep	JPB-Awake
Montage	2.1	2.1	3.1	1.1	1.1
Length	4h	4h	5h10min	4h	4h
No. of seizures	1	1	1	0	0
Seizure index and Occurrence Time	(1) 6:34:01 6:35:32	(2) 8:33:56-8:35:04	(3) 5:16:41-5:18:12	No Seizure	No Seizure

Table 4.2: Patient SB (selected channel: LFC3-LFC5)

Files	SB-SEZ1	SB-SEZ2	SB-SEZ3	SB-Sleep	SB-Awake
Montage	1.1	1.1	2.1	1.1	1.1
Length	4h	4h 14min	4h	4h	4h
No. of seizures	1	1	1	0	0
Seizure index and Occurrence Time	(1) 1:23:03-1:25:17	(2) 7:44:45-7:45:56	(3) 1:55:57-1:57:56	No Seizure	No Seizure

Table 4.3: Patient LAB (selected channel: LA1-LA3)

Files	LAB-SEZ1	LAB-SEZ2	LAB-SEZ3	LAB-Sleep	LAB-Awake
Montage	2.1	2.1	2.1	1.1	1.1
Length	4h	4h	4h	4h	4h
No. of seizures	2	1	3	0	0
Seizure index and occurrence time	(1) 23:24:01-23:26:03 (2) 23:45:53-23:48:02	(3) 13:00:26-13:02:18	(4) 16:19:22-16:21:24 (5) 16:55:10-16:56:59 (6) 18:30:24-18:32:31	No seizure	No seizure

Table 4.4: Patient PAS (selected channel: LS4-LS5)

Files	PAS-SEZ3	PAS-SEZ4	PAS-SEZ4A	PAS-Sleep	PAS-Awake
Montage	4.1	4.1	3.1	3.1	3.1
Length	4h	4h	4h	4h	4h
No. of seizures	1	3	2	0	0
Seizure index and Occurrence Time	(1) 15:01:29-15:01:40	(2) 23:06:35-23:06:45 (3) 23:14:09-23:14:23 (4) 23:38:40-23:38:52	(5) 10:33:41-10:34:00 (6) 11:38:34-11:38:47	No Seizures	No Seizures

Table 4.5 : Patient LAM [selected channel: LP1-LP3 (Type I), LP7-LP9(Type II)]

Files	LAM-SEZ1	LAM-SEZ2	LAM-SEZ3	LAM-Sleep	LAM-Awake
Montage	3.2	3.2	3.2	2.2	3.2
Length	4h	4h	4h	4h	4h
No. of Seizures	1	11	2	0	0
Seizure Index and Occurrence Time	(1) 18:58:33-18:59:17 (I)	(2) 3:14:21-3:15:11 (I) (3) 3:28:31-3:29:02 (I) (4) 3:49:55-3:50:53 (I) (5) 3:56:30-3:57:07 (I) (6) 4:06:46-4:07:28 (I) (7) 4:08:48-4:09:05(II) (8) 4:11:48-4:12:05(II) (9) 4:19:50-4:20:50 (I) (10) 4:23:59-4:24:17 (II) (11) 4:27:36-4:27:54 (II) (12) 4:30:11-4:30:31 (II)	(13) 13:19:57-13:20:38 (I) (14) 14:04:37-14:05:02 (I)	No seizures	No seizures

Among the five patients, patients JPB, SB and LAB all have very long generalized seizures. The seizures are longer than 1 minute and the activities are rhythmic with sustained large amplitude. The morphology of seizures in each patient is very similar. The cases of patients PAS and LAM are more complicated: both of them have focal seizures occurring only in a few channels. Patient PAS has very short seizures, with length no longer than 20 seconds, and the amplitude of the seizure activity is not high.

Patient LAM has two types of seizures. Type I seizures are characterized by intermittent activity of mixed frequencies and Type II seizures are very short seizures. Both types of seizure activities are not very rhythmic. Therefore, we divide the five patients into three cases: patients JPB, SB and LAB as Case 1, patient PAS as Case 2 and patient LAM as Case 3. Next we will discuss the detection results of the three cases separately.

4.2.2 Results

As described in Chapter 3, in our model-based seizure detection method, the seizure estimation from the observed EEG is first performed using the derived model in the context of SONF, and then the energy ratio (γ') between the estimated seizure and the observed EEG calculated. A 24 point moving average smoothing is applied to the energy ratio to get γ. As mentioned earlier, the final seizure detection criterion δ is defined as the difference between the averaged γ value in a test window and that of the background window (Figure 3.5). By setting a proper threshold δ_{TH} for δ, we can decide as to whether a seizure is present or not. As stated in Chapter 3, all detections that occur within 30s of each other are grouped and considered as one seizure activity.

We use two statistical measures – sensitivity (detection rate) and false detection rate to evaluate the model-based seizure detection method. Sensitivity (detection rate) is defined as the ratio of the number of true detections to the total number of seizures identified by the EEG expert; false detection rate is defined as the number of false detections per hour.

(1) Case 1: Patients JPB, SB and LAB

For patients in Case 1, all the seizures are longer than 1 minute. Hence, only the first minute of each selected seizure is taken as the *template seizure*. From a single channel of

the *template seizure*, three stationary *template epochs* are selected visually. Each epoch is 6 seconds long in duration.

For patient JPB, the No.1 seizure (6:34:01-6:35:32) in file JPB-SEZ1 is used to derive the seizure model. The *template seizure* and the *template epochs* are shown in Figure 4.15.

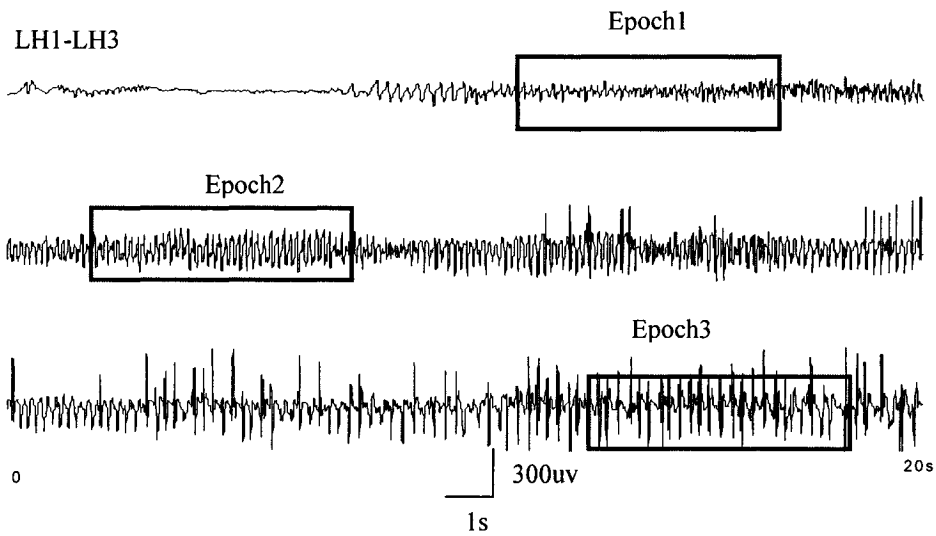

Figure 4.15 The template seizure and the three template epochs of patient JPB

For patient SB, the No.1 seizure (1:23:03-1:25:17) in file SB-SEZ1 is used to derive the seizure model. The *template seizure* and the *template epochs* are shown in Figure 4.16.

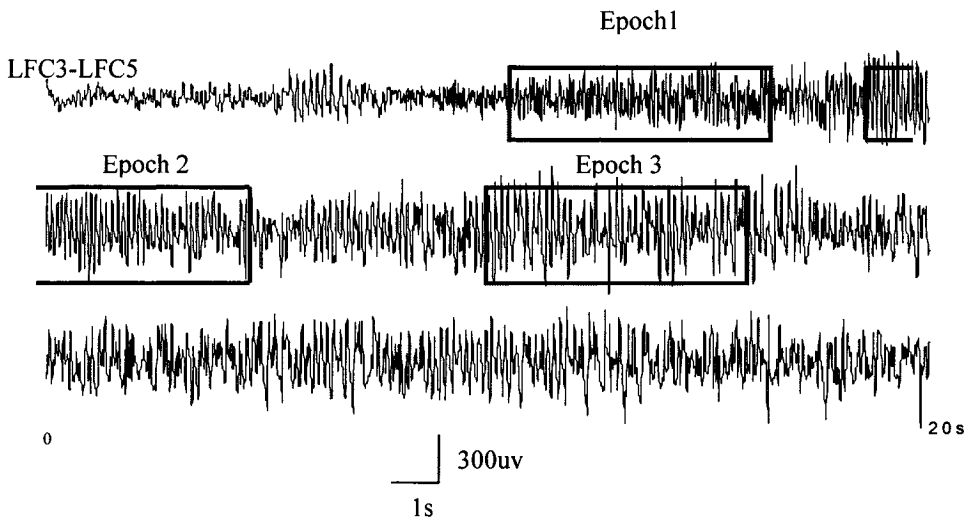

Figure 4.16 The template seizure and the three template epochs of patient SB

For patient LAB, the No.1 seizure (23:24:01-23:26:03) in file LAB-SEZ1 is used to derive the seizure model. The *template seizure* and the *template epochs* are shown in Figure 4.17.

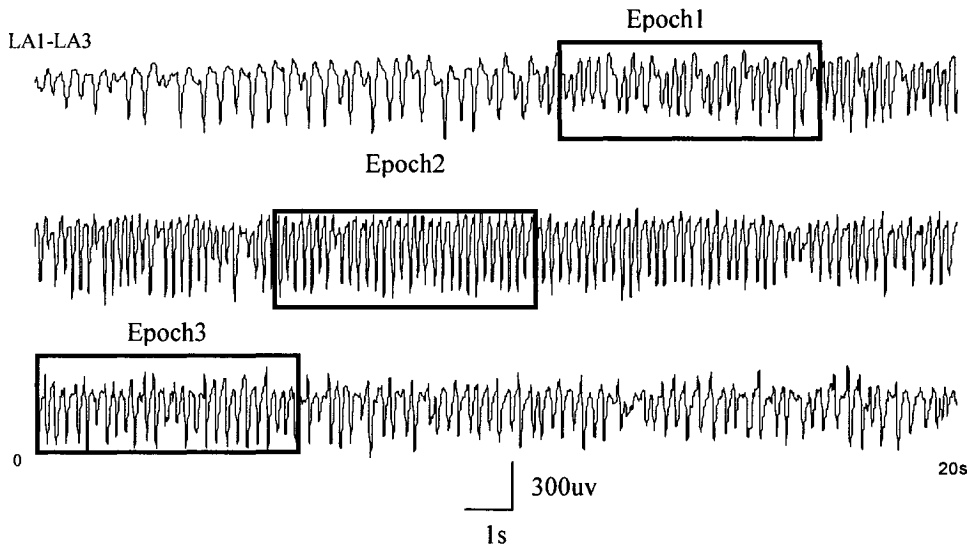

Figure 4.17 The template seizure and the three template epochs of patient LAB

Basis functions are then derived from the *template epochs* using Method 4 (SWBF). Threshold values are calculated using the method described in Chapter 3. For patient JPB, δ_{TH} =0.14; for patient SB, δ_{TH} =0.18; for patient LAB, δ_{TH} =0.18.

The five data files (about 20 hours) of each patient are then processed by the model-based seizure detection method as described in Chapter 3.

Figures 4.18–4.23 show some examples of the detected seizures, and the γ and δ distributions.

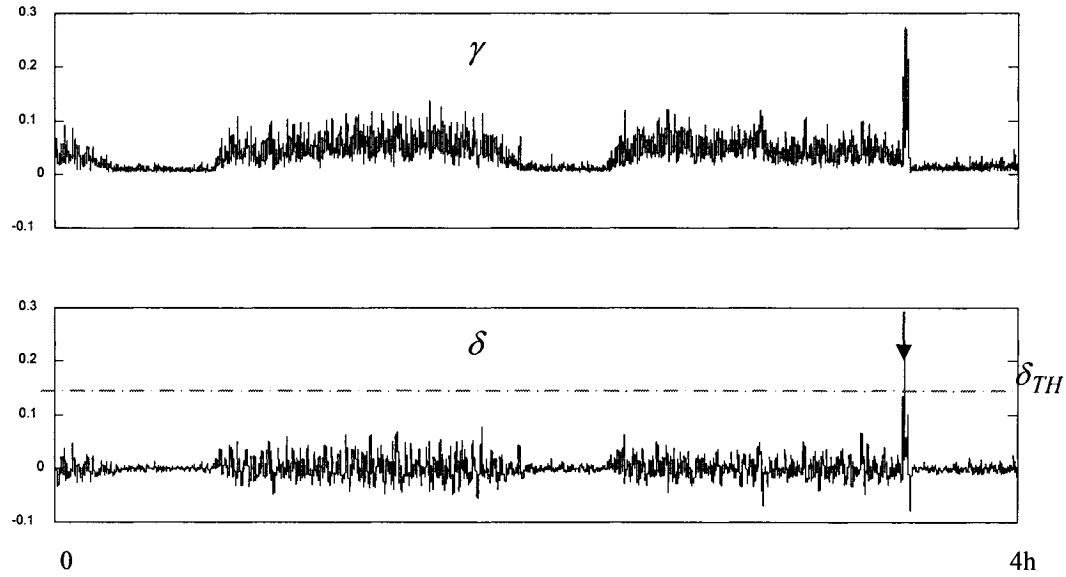

Figure 4.18 γ and δ distributions of file SB-SEZ2 (Seizure No.2). The arrow indicates the seizure location. The dash-dot line indicates the threshold

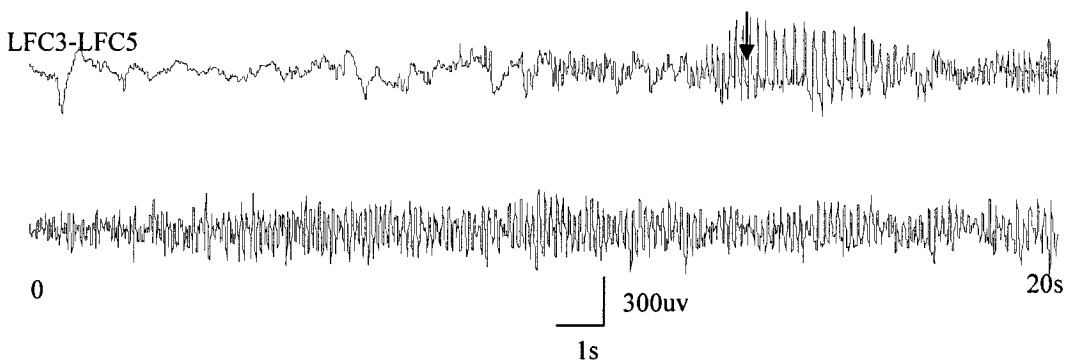

Figure 4.19 Detected seizure in file SB-SEZ2 (Seizure No.2). The arrow indicates the first detection.

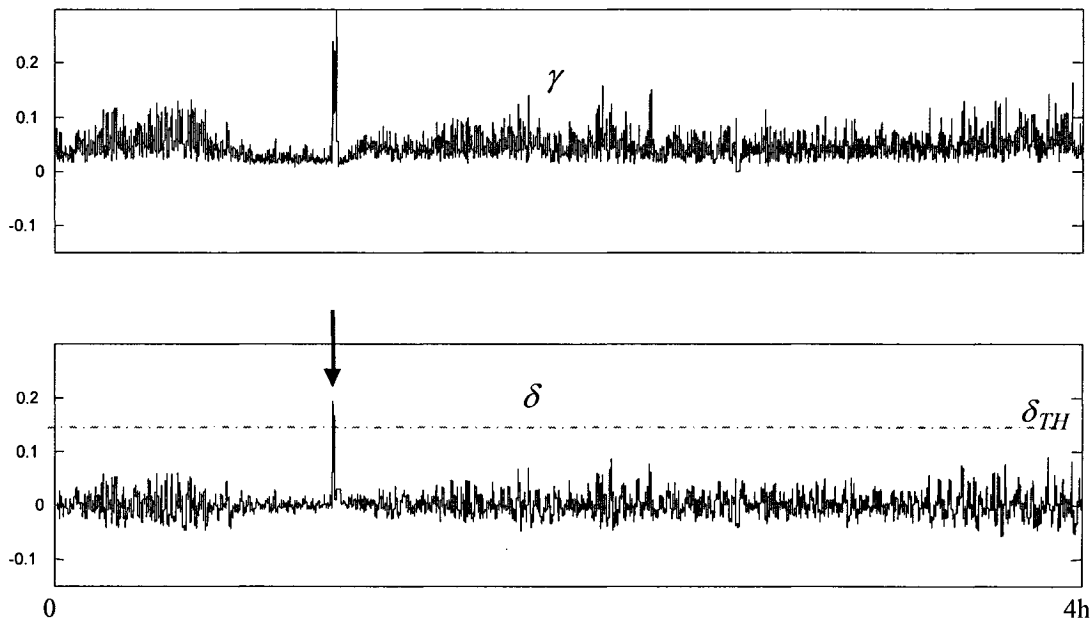

Figure 4.20 γ and δ distributions of file JPB-SEZ2 (Seizure No.2). The arrow indicates the seizure location. The dash-dot line indicates the threshold.

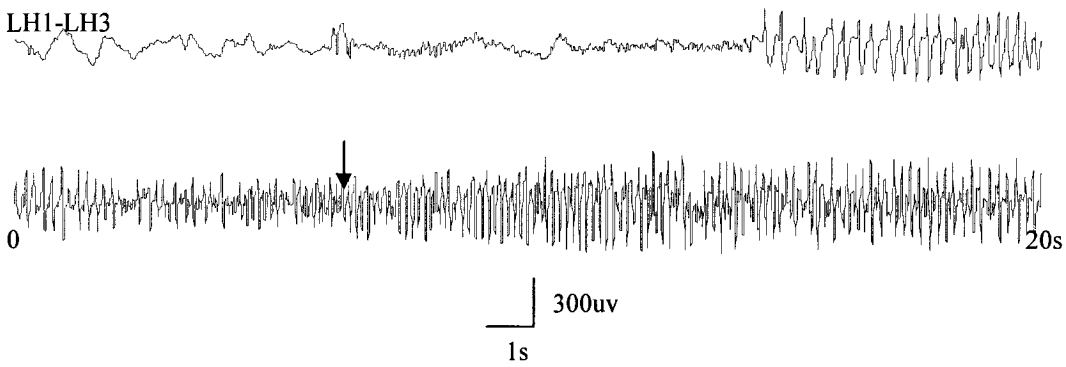

Figure 4.21 Detected seizure in file JPB-SEZ2 (Seizure No.2). The arrow indicates the first detection.

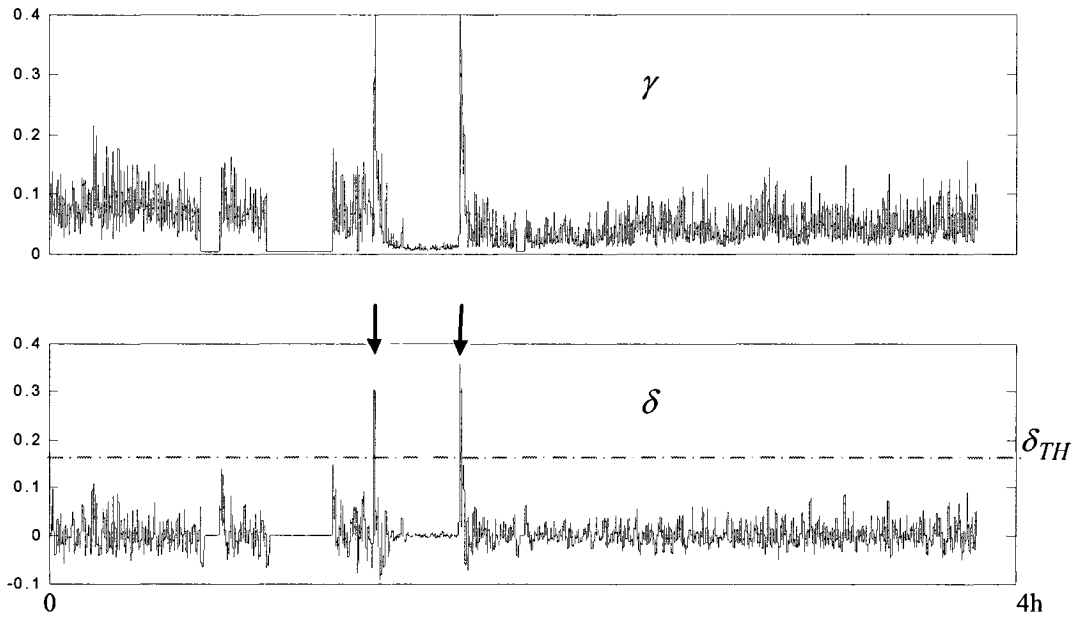

Figure 4.22 γ and δ distributions of file LAB-SEZ1 (Seizure No.1 &2). The arrows indicate the seizure locations. The dash-dot line indicates the threshold.

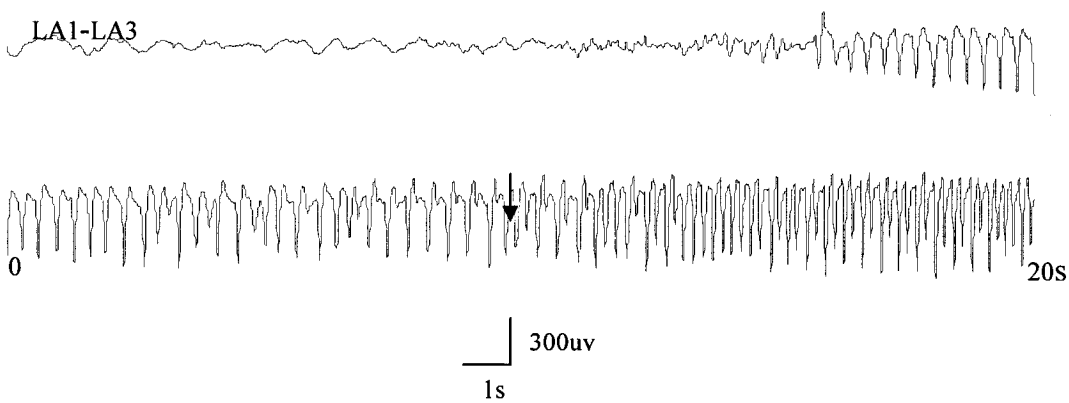

Figure 4.23 Detected seizure in file LAB-SEZ1(Seizure No.2). The arrow indicates the first detection.

From these figures, we can see that γ and δ values at the seizure locations are greater than those for the background EEG, making it easy for true detections to happen.

The twelve seizures in the three patients (JPB, SB and LAB) share some common characteristics. All of the twelve seizures are generalized seizures (a generalized seizure means seizure occurs in many channels). Seizure amplitudes are high and durations are long, and seizure activities are very rhythmic. Moreover, in each of the three patients, the *template seizure* and other seizures in the patient resemble one another in morphology to a great extent. For this kind of seizures, the model-based seizure detection method using SONF shows perfect result. For the three selected patients, the sensitivity is 100% and the false detection rate is 0/hour. Table 4.6 summarizes the detection results for Case 1.

Table 4.6 Detection results for Case1 (Patients JPB, SB and LAB).

Patient	Hours	Number of Seizures (non-template seizures)	True Detections	False Detections	Sensitivity	False Detection Rate
JPB	21	2	2	0	100%	0.0/hour
SB	20	2	2	0		
LAB	20	5	5	0		

(2) Case 2: Patient PAS

There are 5 visually identified seizures in patient PAS. Additionally, upon review of the data, it was realized that there is one very distinct seizure that was missed by the expert. Clearly, this is a true seizure and we therefore include it in the manually identified seizure

group. All the 6 seizures are focal seizures occurring only in a few channels and are shorter than 20 seconds.

The No.1 seizure in PAS-SEZ3 (15:01:29-15:01:40) is used as the *template seizure*. Only one *template epoch* (6 seconds long) is selected from the *template seizure* because of its short duration. Figure 4.24 shows the *template seizure* and the *template epoch*.

Basis functions are then derived from the *template epoch* using Method 4—Sinusoidal Wavelet Basis Functions. Threshold is calculated using the method described earlier. For patient PAS, δ_{TH} =0.035. The five data files (about 20 hours) of patient PAS are then processed by the model-based seizure detection method.

Figures 4.25 shows one example of the γ and δ distributions, and Figure 4.26 shows one example of a detected seizure.

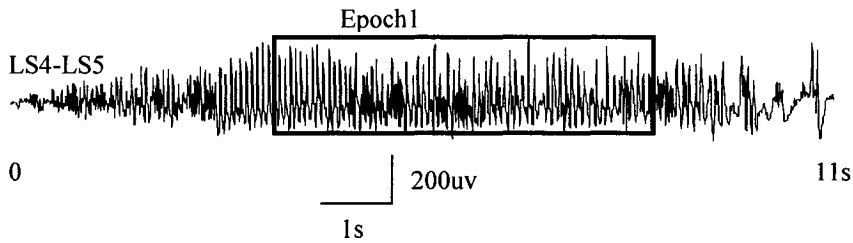

Figure 4.24 The template seizure and the template epoch of patient PAS. Only one template epoch is selected because of the short duration of the template seizure.

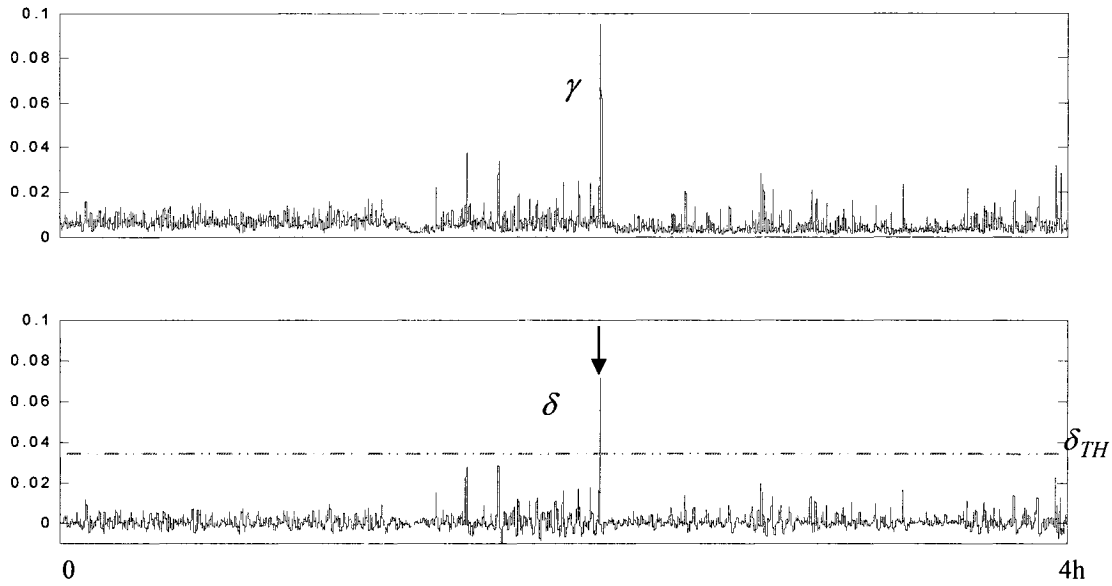

Figure 4.25 γ and δ distributions of file PAS-SEZ4 (Seizure No.4). The arrow indicates the seizure location. The dash-dot line indicates the threshold.

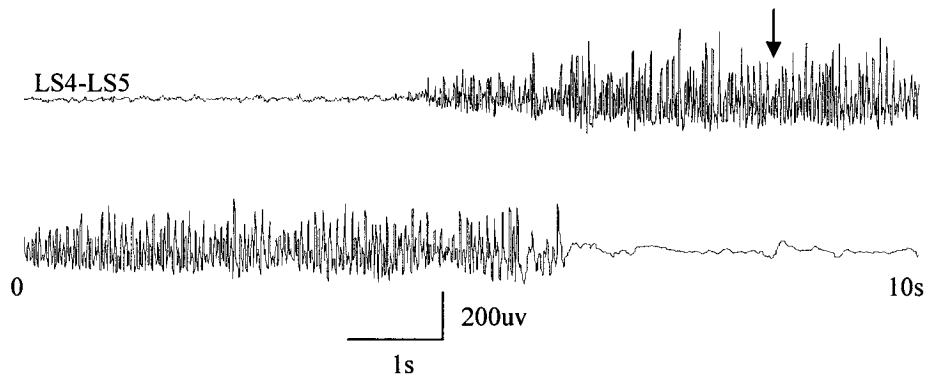

Figure 4.26 The detected seizure in file PAS-SEZ4 (Seizure No.4)

Generally speaking, the detection result for patient PAS is not so satisfactory as for the patients in Case 1. A total of 5 seizures have been detected, with 2 true detections and 3

false detections. Three seizures have been missed. Table 4.7 summarizes the detection result for patient PAS.

Table 4.7 Detection result for Case 2 (patient PAS).

Patient	Hours	Number of Seizures (non- template seizures)	True Detections	False Detections	Sensitivity	False Detection Rate
PAS	20	5	2	3	40%	0.15/hour

(3) Case 3: Patient LAM

The case of patient LAM is much more complicated than Case 1 or Case 2. There are 14 seizures in the five files of patient LAM. They are all focal seizures occurring only in a few channels and can be classified into two types according to their morphologies. Type I seizures are characterized by intermittent activity of mixed frequencies and Type II seizures are very short seizures. Unlike seizures in Case 1 or Case 2, seizure activities in this patient are not very rhythmic. No sustained rhythm can be found during a seizure. Background EEG is also complicated as it contains considerable interictal epileptic activity. Waveforms such as bursts of spike or spike and wave, short burst of rhythmic activities frequently appear in the background EEG.

We take the No.3 seizure (occurring from 3:28:31-3:29:02) in LAM-SEZ2 as the template seizure for Type I seizures. Channel LP1-LP3 (Montage 3.2) is selected since seizure activity is most prominent in this channel for Type I seizures. Only two *template epochs* are selected because only two relatively rhythmic epochs can be found during the

template seizure. Figure 4.27 shows the *template seizure* and the two selected *template epochs* for Type I seizures.

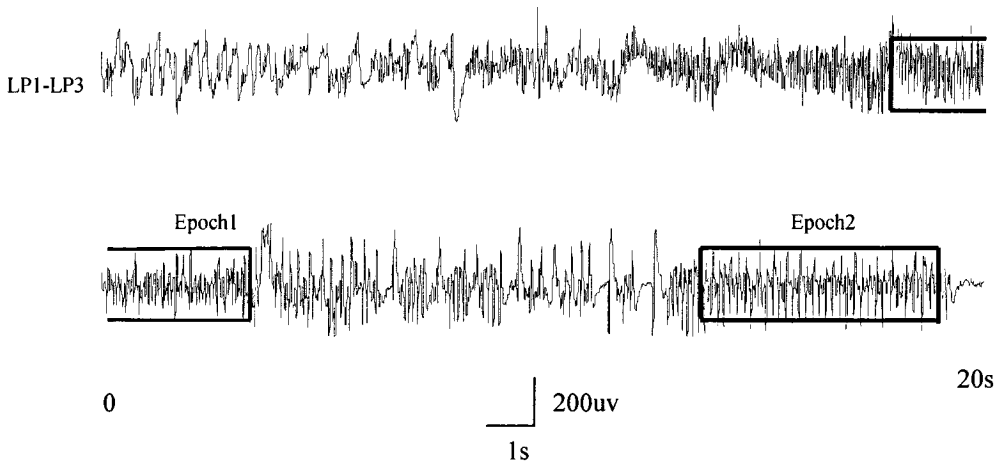

Figure 4.27 The template seizure and the two template epochs for Type I seizures in patient LAM

For Type II seizures, we take No.7 seizure (occurring from 4:08:48-4:09:05) in LAM-SEZ2 as the template seizure. Channel LP7-LP9 (Montage 3.2) is selected since seizure activities are most prominent in this channel for Type II seizures. Only one template epoch is selected. Figure 4.28 shows the template seizure and the selected *template epoch* for type II seizures.

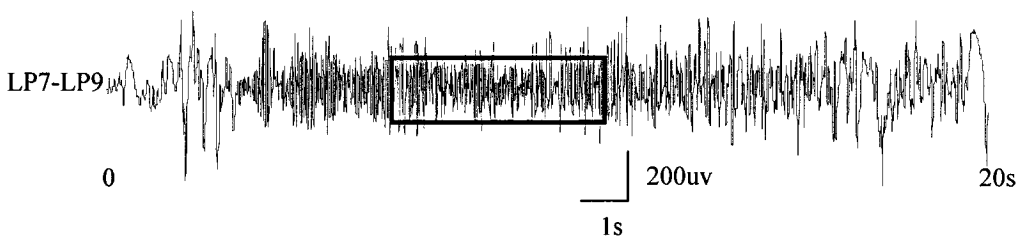

Figure 4.28 The template seizure and the template epoch for Type II seizure in patient LAM

In the initial evaluation, we set the length of the template epochs in patient LAM as 6 seconds, the same as in the other two cases. Basis functions are then derived from the *template epochs* using Method 4—SWBF. The data files of patient LAM are then processed using the model-based seizure detection method. The results are not satisfactory: seizure and non-seizure activities cannot be distinguished from the γ or δ distributions.

By studying the selected *template epochs* in Figures 4.27 and 4.28 carefully, we find that the 6s *template epochs* are not adequate for this patient. As stated earlier, seizure activities in patient LAM are intermittent and with mixed frequencies and not very rhythmic. During the evolvement of the seizure, frequencies change rapidly and no sustained rhythm can be found. For the current modeling method, the *template epochs* in all the patients are selected to be 6 seconds in duration; however for patient LAM, no rhythm is sustained for as long as 6 seconds. Therefore, we re-adjust the lengths of the *template epochs* according to the characteristics of the two *template seizures.*

For Type I seizures, the new *template epochs* in the *template seizure* are chosen to be 3 seconds long and two epochs are selected. Figure 4.29 shows the *template seizure* and the newly selected *template epochs* for Type I seizures.

New basis functions are then generated from the new *template epochs* using Method 4 (SWBF). The model-based seizure detection method is then applied to the data files of patient LAM using the new basis functions.

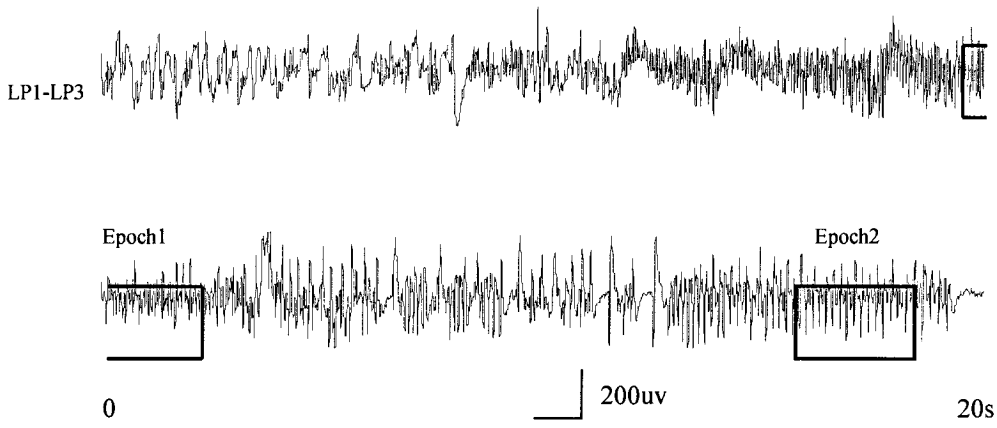

Figure 4.29 The template seizure and the new template epochs for type I seizures in patient LAM

Two examples are presented to show the comparisons (γ' and γ distributions) of using 6s *template epochs* and the 3s *template epochs* for Type I seizures. Figures 4.30-4.31 show the comparisons around the Type I *template seizure*, and Figures 4.32-4.33 show the comparisons around seizure No. 6 (Type I).

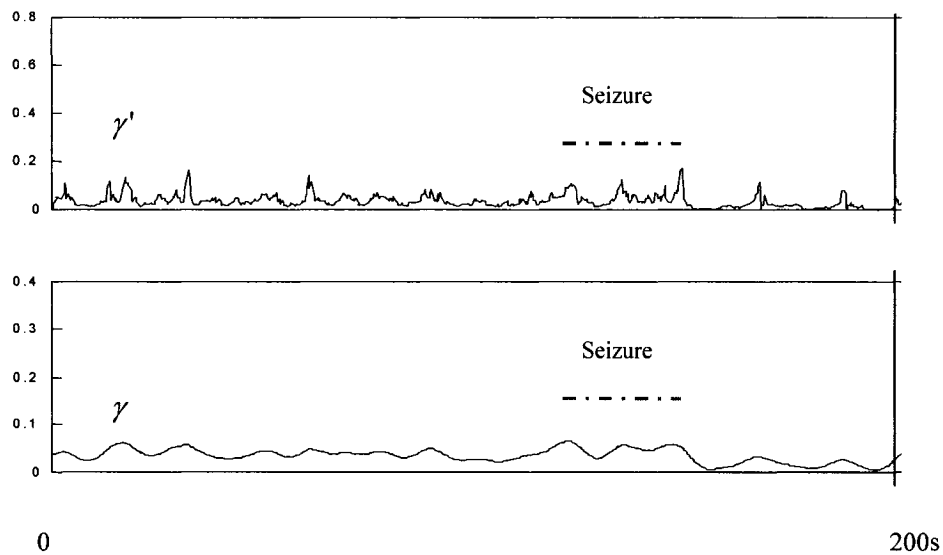

Figure 4.30 γ' and γ distributions around the template seizure (Type I) using the 6s template epochs. Seizure cannot be distinguished from the γ (γ') distributions.

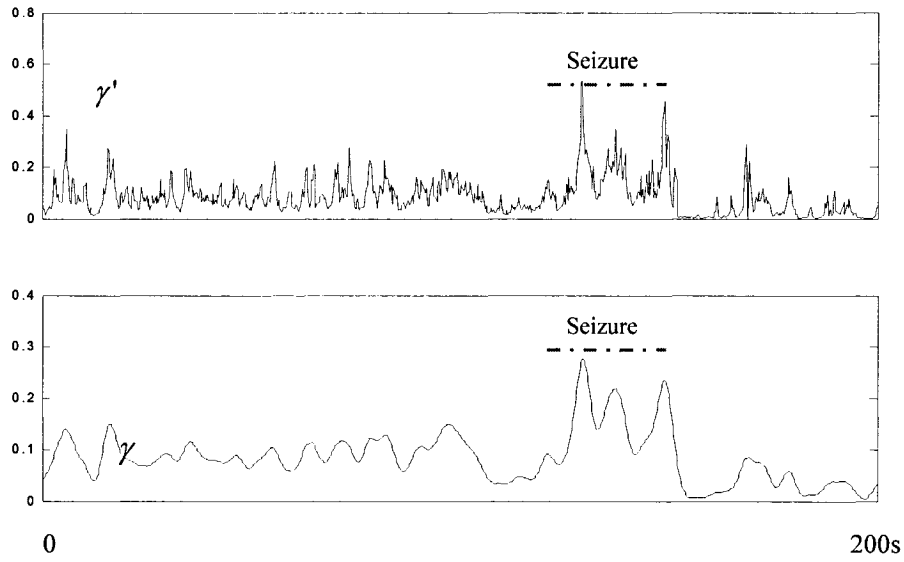

Figure 4.31 $\gamma'$and γ distributions around the template seizure (Type I) using the 3s template epochs. γ (γ') has shown some increase during the seizure time.

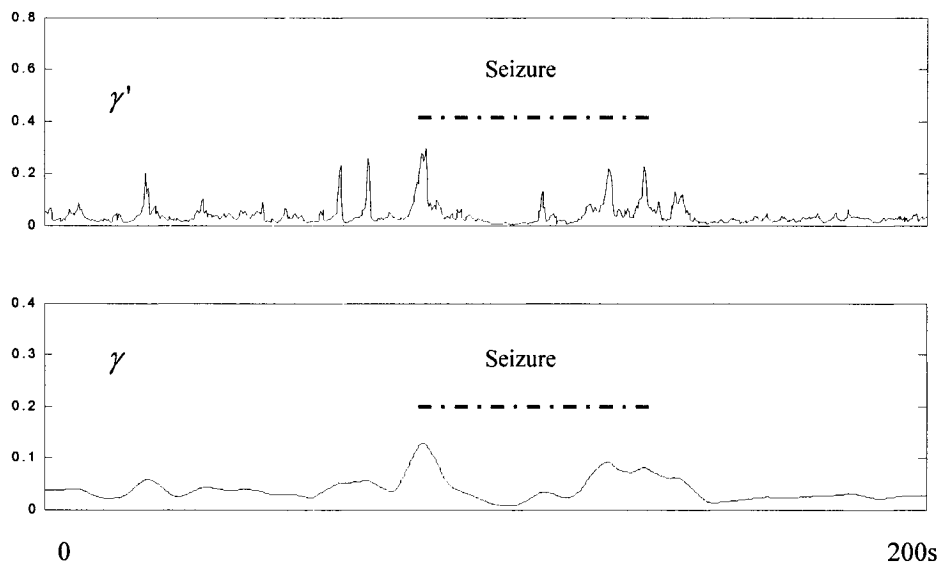

Figure 4.32 $\gamma'$and γ distributions around the No.6 seizure (Type I) using the 6s template epochs. γ (γ') values are not very high during the seizure time.

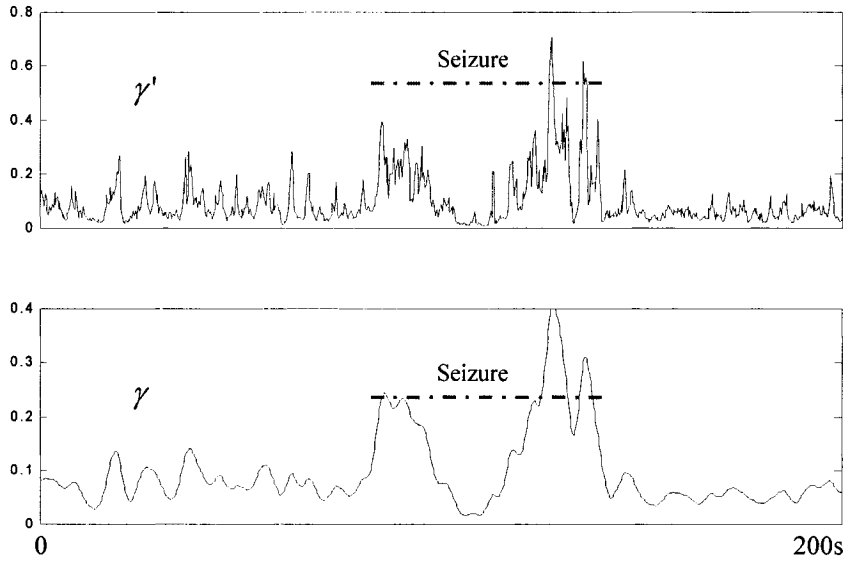

Figure 4.33 γ' and γ distributions around the No.6 seizure (Type I) using the 3s template epochs. $\gamma(\gamma')$ has shown great increase during seizure time.

From Figures 4.30–4.33, we can see that by using the 3s template *epochs* instead of the 6s *template epochs* to model the *template seizure* of Type I, seizure and non-seizure activities can be differentiated from the $\gamma(\gamma')$ distributions.

The detection result for Type I seizures using the 3s *template epochs* is as follows: a total of 15 seizures are detected, with 7 true detections and 8 false detections. One seizure is missed. The sensitivity is 87.5%, and the false detection rate is 0.4/hour. Table 4.8 lists the detection result for Type I seizures in patient LAM (δ_{TH} =0.11).

Table 4.8 Detection result for Type I seizures in Case 3 (patient LAM)

Patient	Hours	Number of Type I Seizures (non- template seizures)	True Detections	False Detections	Sensitivity	False Detection Rate
LAM	20	8	7	8	87.5%	0.4/hour

For Type II seizures, the new *template epoch* is chosen to be 2 seconds long and only one epoch is selected. Figure 4.34 shows the template seizure and the newly selected *template epoch* for Type II seizures.

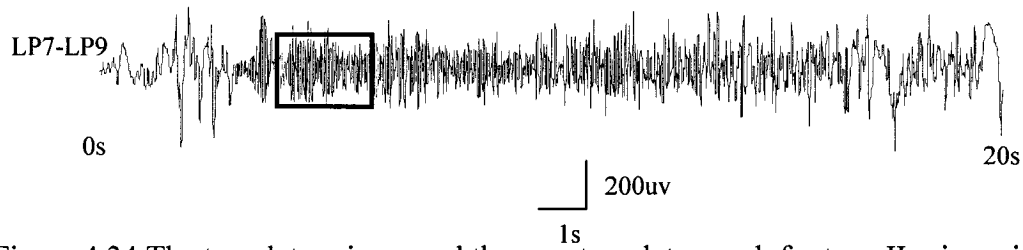

Figure 4.34 The template seizure and the new template epoch for type II seizure in patient LAM

New basis functions are then generated from the new *template epoch* using Method 4 (SWBF). The model-based seizure detection method is then applied to the data files of patient LAM using the new basis functions.

Two examples are presented to show the comparisons ($\gamma'$and γ distributions) using the 6s *template epoch* and the 2s *template epoch* for Type II seizures. Figures 4.35-4.36 show the comparisons around the Type II *template seizure*, and Figures 4.37-4.38 show the comparisons around seizure No.8.

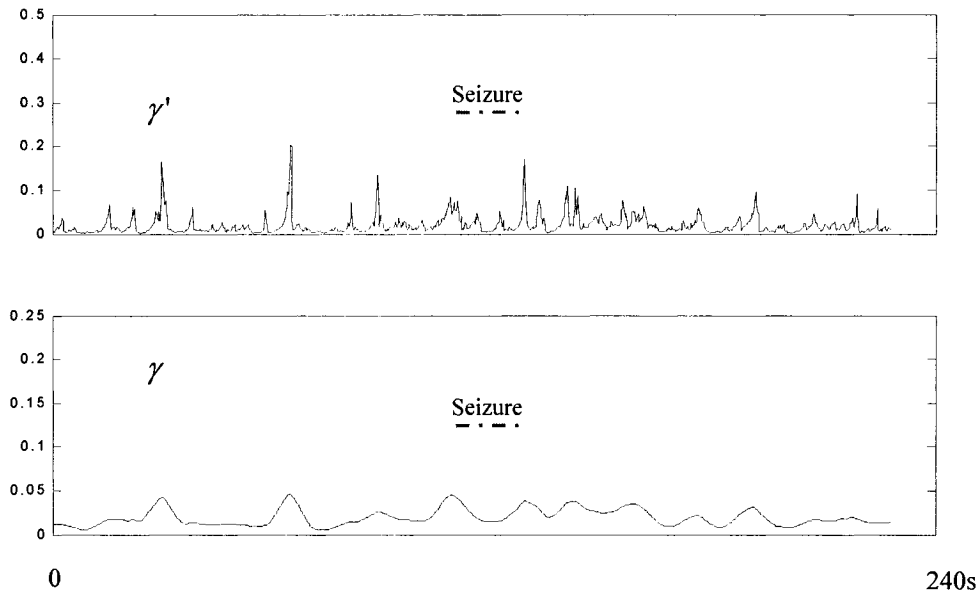

Figure 4.35 $\gamma'$and γdistributions around the template seizure (Type II) using the 6s template epoch. Seizure cannot be distinguished from the $\gamma(\gamma')$ distributions.

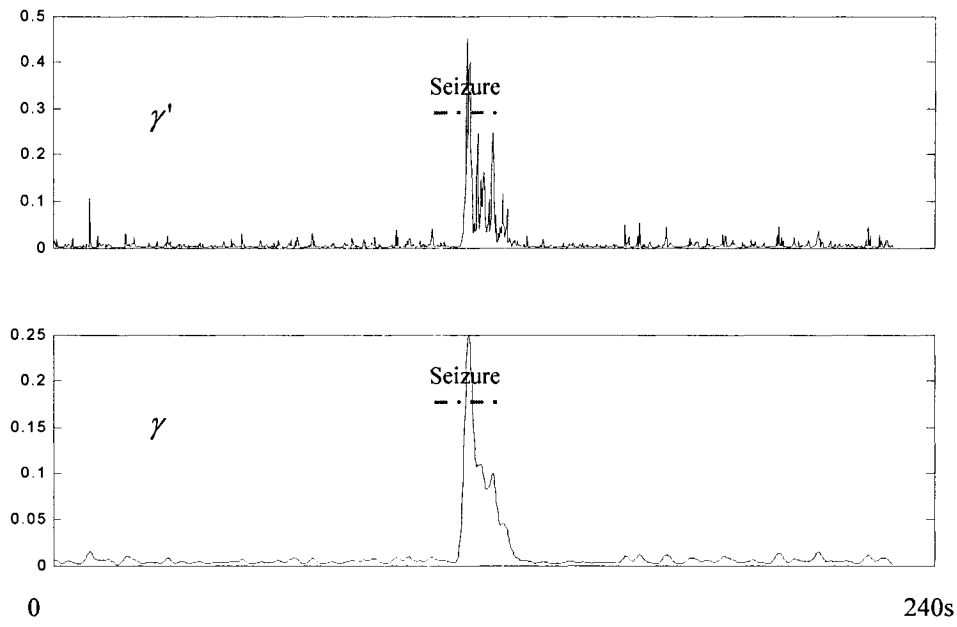

Figure 4.36 $\gamma'$and γdistributions around the template seizure (Type II) using the 2s template epoch. $\gamma(\gamma')$ has shown great increase during seizure time.

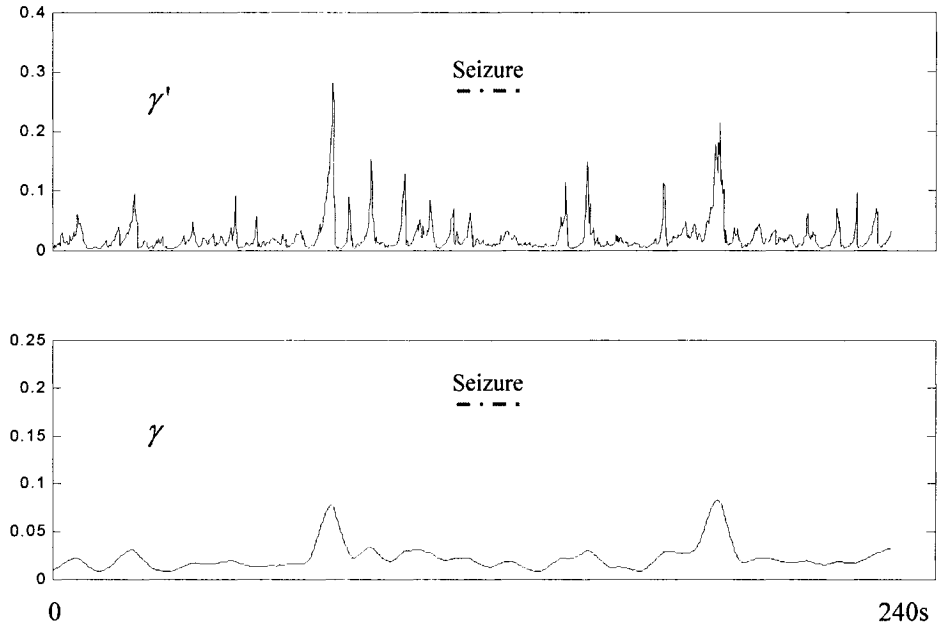

Figure 4.37 $\gamma'$and γ distributions around the No.8 seizure (Type II) using the 6s template epoch. Seizure cannot be distinguished from the $\gamma(\gamma')$ distributions.

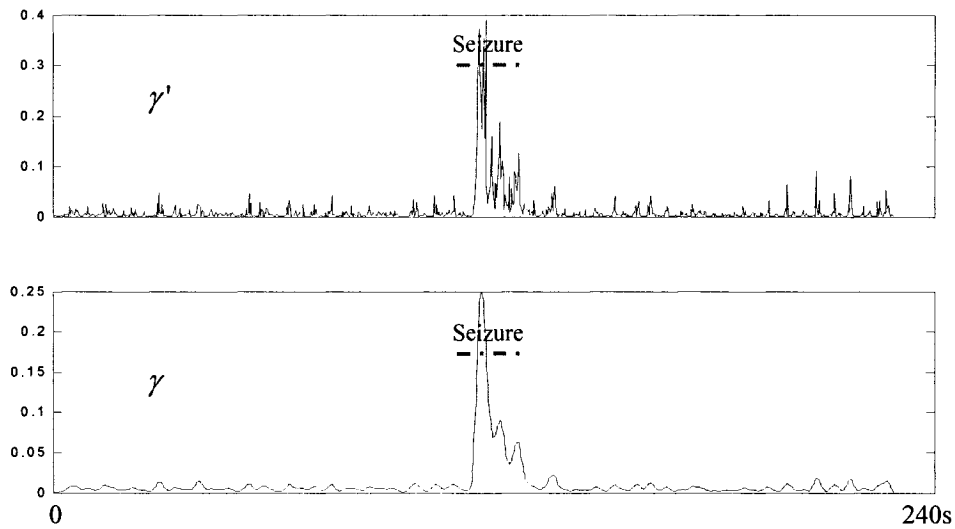

Figure 4.38 $\gamma'$and γ distributions around the No.8 seizure (Type II) using the 2s template epoch. $\gamma(\gamma')$ has shown great increase during the seizure time.

From Figures 4.35-4.38, we can see that by using the 2s template *epoch* instead of the 6s *template epoch* to model the type II *template seizure*, seizure and non-seizure activities can be easily distinguished from the $\gamma(\gamma')$ distributions.

The detection results for Type II seizures using the 2s *template epoch* are as follows: a total of 5 seizures are detected, with 4 true detections and 1 false detection. The sensitivity is 100% and the false detection rate is 0.05/hour. Table 4.9 summarizes the detection result for type II seizures in patient LAM (δ_{TH}=0.1).

Table 4.9 Detection result for Type II seizures in Case 3 (patient LAM)

Patient	Hours	Number of Type II Seizures (non- template seizures)	True Detections	False Detections	Sensitivity	False Detection Rate
LAM	20	4	4	1	100%	0.05/hour

4.3 Discussion

The first automatic seizure detection method to be widely used in clinical setting was that of Gotman [9]. It is based on the general characteristics of the seizures, such as the large amplitude, fast frequency, and rhythmic activity. The combined results of several evaluations show a sensitivity of 70-80% and a false detection rate of 1-3/h. Another notable seizure detection method is that of Gabor [18, 19] based on neural network. The evaluation showed a sensitivity of 92.8%, and a false detection rate of 1.35/h.

The first *patient-specific* automatic *seizure onset* detection system was proposed by Qu and Gotman [4]. It used an existing seizure as the *template* and a large set of background EEG patterns to detect oncoming *seizure onsets* in the same patient.

The purpose of our model-based seizure detection method is to try to improve the sensitivity and lower the false detection rate by using a *model* for each type of seizure. Similar to the method of Qu and Gotman, one *a priori* known seizure is needed as the *template*, from which the *model* is derived using the proposed modeling method. *Statistically optimal null filters* (SONF) are then used to estimate the seizure from the observed EEG. The energy ratio between the seizure estimate and the observed EEG is calculated, processed and used as the criterion to decide if a seizure is present or not. As the first step, we used simulated EEG data to test the proposed six modeling methods. Results show that among the six proposed modeling methods, Method 4 (SWBF) gives the best result. Then, we used the SWBF in our model-based seizure detection method to process the real SEEG data of five patients.

Among the five patients considered, detection results for Case 1 (patients SB, JPB and LAB) are perfect. For the three patients, the sensitivity is 100% and the false detection rate is 0/h. Several reasons can account for the perfect result. First, all the three patients in Case 1 have generalized seizures with long duration--each seizure is longer than 1 minute. The sustained activity enables us to easily select three stationary *template epochs* from the *template seizure*, and increases the possibility of detecting the seizures. That is, if the seizure is missed by the first *template epoch*, there are still chances to detect by the second or third *template epochs*. Seizure activity is very rhythmic, and this satisfies the condition from which the set of basis functions (SWBF) were derived.

Another very important reason is that, in each patient, seizures from their onsets to the later stages resemble the *template seizure* very much. There is a very clear pattern for the seizures in each patient. Based on the above reasons, it is not surprising that perfect results have been obtained for all the three patients in Case 1.

Case 2 (patient PAS) has different kind of seizures from the patients in Case 1. The most prominent characteristic of the seizures in this patient is their short durations. Detection result using our model-based seizure detection method is not satisfactory for this patient. The false detection rate is low, and the sensitivity is also low.

By studying the γ and δ distributions of patient PAS, we found that, if a lower threshold (0.021) is used for this patient, there will be no missed detections. At present, the threshold is set to be the difference between the averaged γ value of the *template seizure* and that of the background (30 seconds before the template seizure), which is 0.035 for this patient. This seems too high for this patient. Even though there are no missed detections for the three patients in Case 1, by studying the γ and δ distributions of the patients we found that there is still room for lowering the thresholds without causing any false detections. The current threshold setting seems to be not optimal. In order to establish more appropriate threshold setting strategy, it is necessary to use a large training data set. In the future, more training data should be used to find the optimal threshold.

The false detections in patient PAS are caused by some high-amplitude artifacts at the start of some of the EEG segments. Figure 4.39 shows one example of such an EEG segment and the corresponding seizure estimate using SONF from this segment.

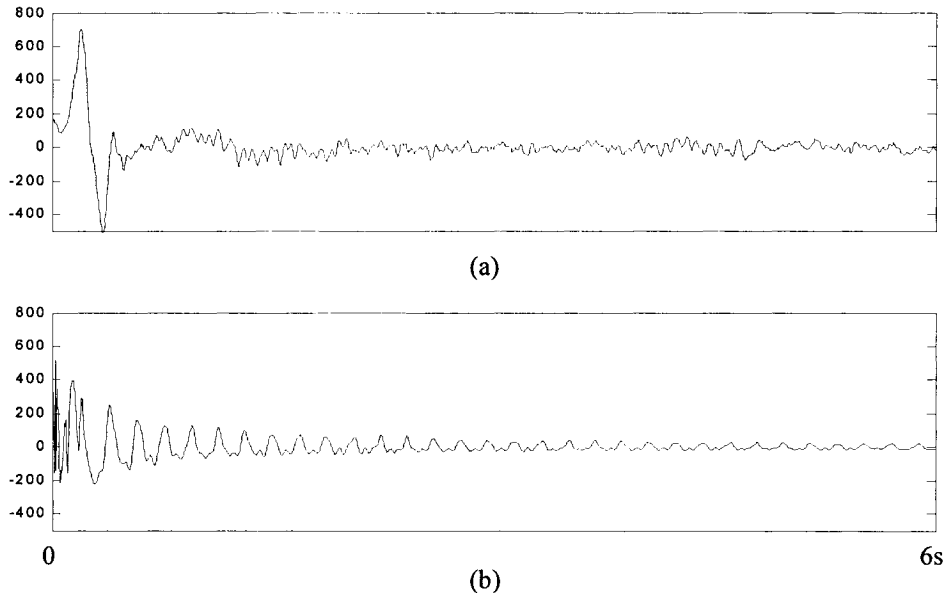

Figure 4.39 EEG segment with artifact at start and its seizure estimate (a) EEG segment with artifact at start. (b) seizure estimate from the EEG segment.

From Figure 4.39, we can see that the output of the SONF cannot track the input properly at this situation. At the start, the input (high-amplitude artifact) has some identical frequency components as the basis functions, therefore the output of the SONF has the same frequency components. But when the artifact is over, even though the input does not contain any frequency components that match the basis functions, the output cannot track the change fast enough. The energy ratio of the output and input will be large in this situation, making it possible for a false detection to occur. More detailed explanations via simulation are described in the Appendix. In the future, this problem may be resolved by identifying and rejecting the artifact in the EEG segments first.

The processing results of patient LAM (Case 3) using 6s *template epochs* show that the model-based seizure detection method is not effective: seizure and non-seizure

activities cannot be distinguished from the γ or δ distributions. The reason for the ineffectiveness is that the 6s template epoch is too long for this patient, since no rhythm is sustained for as long as 6 seconds in patient LAM. By using shorter *template epochs* (3s for type I seizures and 2s for type II seizures), detection results have improved significantly for both types of seizures. Hence, when selecting the *template epochs* to model the *template seizure*, it is very important to choose the length of the *template epochs* according to the characteristics of the *template seizure* rather than fix the length for all patients. In the future, some automatic segmentation techniques that divide the *template seizure* into several stationary segments may be used to help in the selection of the *template epochs*.

There is one missed detection (seizure No.5, Type I) in patient LAM. Checking the missed seizure in the selected channel LP1-LP3, we found that the morphology of the seizure in this channel does not match the template seizure. It is therefore reasonable that the method is not able to detect this seizure.

The false detections in patient LAM are caused by the same reason as in Case 2: some high-amplitude, short-duration artifacts occur frequently in the channel LP1-LP3. Artifact rejection is needed to solve this problem in the future.

For most of the seizure detection methods, short burst of rhythmic activity, rapid eye blinking and EMG artifact caused by chewing are the main reasons that cause false detections [8, 9, 10]. For our method, even if these activities exist, they are not likely to match the *model* derived from the template seizure, and therefore false detection will not occur. Compared to the other seizure detection methods, our model-based seizure

detection method may lower the false detection rate, and the detection results of the five patients suggest this to be the case.

Chapter 5

Conclusion

About 0.5-1% of the population suffer from epilepsy, which is the most common neurological disease next to strokes [1]. The manifestations of epilepsy are bursts of seizures and spikes, which are defined as abnormal EEG patterns.

Nowadays, long-term EEG monitoring with video is being used in clinics to capture seizures in epilepsy patients. It can provide the combined information about the clinical and electrographic seizures, and it is more likely to capture epileptiform abnormalities (for example, seizures) than a short-term recording. However, it is difficult for the neurologists to observe a seizure closely or to interact continuously with the patient, since the EEG monitoring sessions can last from several days to weeks [4]. Automatic seizure detection is thus necessary in the long-term EEG monitoring process.

Several automatic seizure detection methods have been developed since 1970. Some are based on general seizure characteristics, such as large amplitude, high frequency, rhythmic activity and so on, while others are based on neural networks or wavelet transforms. Performance (for example, sensitivity and false detection rate) of these methods varies significantly.

In this thesis, we have tried to address the problem of automatic seizure detection in a way that is different from the traditional seizure detection methods. The traditional seizure detection methods usually extract some general features of the seizures, such as average amplitude and average frequency. Detection criterion is developed using these features. Our *model-based seizure detection method using the statistically optimal null filters (SONF)* performs customized detections for each patient through the use of the patient's own *a priori* known seizure as a detection *template*. Subsequent EEG recordings

of the same patient are processed using the SONF, which was proposed for solving the problems of estimating short-duration signals embedded in noise. The output of the SONF represents the noise-free estimate of the seizure. A detection criterion using the estimated seizure and the observed EEG is developed for the final seizure detection method.

In Chapter 1, we introduced some basic concepts such as what EEG is and what seizure is, and reviewed some of the seizure detection methods in the literature. In Chapter 2, we described the principle of the SONF, then introduced several kinds of SONF, and presented an example of using SONF for the estimation of a signal embedded in noise. In Chapter 3, we presented the *model-based seizure detection method using SONF*, and proposed six methods of modeling the template seizure — constructing basis functions that are needed to implement the SONF in the *model-based seizure detection method.* In Chapter 4, we first used simulated EEG data to find the optimal basis functions from the proposed six modeling methods. Then we used the SEEG data of five patients to develop and test the model-based seizure detection method using SONF. Simulation results show that, modeling using Method 4 (Sinusoidal wavelet basis functions) has a better performance than the other modeling methods. The processing results of the SEEG data of the five patients show that the model-based seizure detection method using SONF can lower the false detection rate, and is most effective for long rhythmic seizures with a clear pattern. Besides, it is very important to select the length of the *template epochs* according to the characteristics of the seizure rather than to use a fixed length for all patients.

There still remains considerable work to be done to improve the method, such as using spatial information from multi-channels instead of using the information from only one channel; using more training data to find the optimal detection threshold for each patient and selecting the length of the *template epochs* adaptively according to the characteristics of the *template seizure* instead of using a fixed length.

Main Contributions

The main contributions of the thesis may be summarized as follows:

1. A new seizure detection method (*model-based seizure detection method using the SONF*) has been proposed. This method utilizes an *a priori* known seizure as a *model* to detect the subsequent seizures that are similar to the model.
2. Six methods of modeling the template seizure (generating basis functions that are needed in the SONF) have been developed.
3. Simulation has been performed to test the performance of the proposed six modeling methods. Results have shown that Method 4 (SWBF) has a better performance than the other five modeling methods.
4. Real SEEG data of five patients have been processed to develop and test the model-based seizure detection method using the SONF. The results have indicated that this method can lower the false detection rate, and is most effective for long rhythmic seizures with a clear pattern.

Future work

Future work could be carried out on the following aspects:

1. Visually selecting stationary epochs from the template seizure can be replaced by a more precise automatic selection procedure. By using automatic segmentation, the length of the *template epochs* can be determined automatically according to the characteristics of the template seizure. Moreover, by using automatic segmentation, the model-based seizure detection method can eliminate the necessary human intervention to achieve a fully automatic seizure detection method.
2. The information of only one channel has been used in our model-based seizure detection method. In the future, spatial information from multi- channels must be incorporated in the detection scheme. This will further help to enhance a true detection and to reduce a false detection.
3. The current setting of the threshold seems to be not optimal. In order to establish more appropriate threshold setting strategy, it is necessary to use a large training data set. In the future, more training data should be used to find the optimal threshold.
4. Variable length *template epochs* are recommended for different patients according to the characteristics of the template seizure. This may be achieved by using automatic seizure segmentation methods.
5. More EEG data must be used to train/develop the model-based seizure detection method using SONF.

References

[1] F. Wendling, J. Bellanger, et.al., "Extraction of spatio-temporal signatures from depth EEG seizure signals based on objective matching in warped vectorial observations," IEEE Trans. On Biomedical engineering, vol. 43, no. 10, pp. 990-1000, 1996.

[2] David E. Blum, "Computer-based electroencephalography: technical basics, basis for new applications and potential pitfalls," Electroenceph. Clin. Neurophysiol., vol. 106, pp. 118-126, 1998.

[3] Christophe C. Jouny, Piotr J. Franaszczuk, Gregory K. Bergey, "Characterization of epileptic seizure dynamics using Gabor atom density," Clinical Neurophysiology, vol. 114, pp. 426-437, 2003.

[4] Hao Qu and Jean Gotman, "A patient-specific algorithm for the detection of seizure onset in long-term EEG monitoring: possible use as a warning device," *IEEE Trans. Biomed. Eng.*, vol. 44, no. 2, pp. 115-122, 1997.

[5] John R. Glover, "Context-based automated detection of epileptogenic sharp transients in the EEG: elimination of false positives," *IEEE Trans. Biomed. Eng.*, vol. 36, no. 5, pp. 519-527, 1989.

[6] S. G. Wilson, M. L. Scheuer et al., "Seizure detection: correlation of human experts, Clinical Neurophysiology," vol. 114, pp. 2156-2164, 2003.

[7] W. E. Hosteler, H. H. Doller, R. W. Homan, "Assessment of a computer program to detect epileptiform spikes," Electroenceph. Clin. Neurophysiol., vol. 83, pp. 1-11, 1992.

[8] J. Gotman, "Automatic detection of seizures and spikes," *Journal of Clinical Neurophysiology,* vol. 16, no. 2, pp. 130-140, 1999.

[9] J. Gotman, "Automatic recognition of epileptic seizures in the EEG," Electroenceph. Clin. Neurophysiol., vol. 54, pp. 530-540, 1982.

[10] Y. U. Khan and J. Gotman, "Wavelet based automatic seizure detection in intracerebral electroencephalogram," Clinical Neurophysiology, vol. 114, pp. 898-908, 2003.

[11] F. Pauri, et al., "Long term EEG video-audio monitoring: computer detection of focal EEG seizure patterns," Electroenceph. Clin. Neurophysiol., vol. 82, pp. 1-9, 1992.

[12] M.C. Salinsky, "A practical analysis of computer based seizure detection during continuous video-EEG monitoring," Electroenceph. Clin. Neurophysiol., vol. 103, pp. 445-449. 1997.

[13] J. Gotman, "Automatic seizure detection: improvements and evaluation," Electroenceph. Clin. Neurophysiol., vol. 76, pp. 317-324, 1990.

[14] Hao Qu and J. Gotman, "Improvement in seizure detection performance by automatic adaptation to the EEG of each patient," Electroenceph. Clin. Neurophysiol., vol. 86, pp. 79-87, 1993.

[15] G. W. Harding, "An automated seizure monitoring system for patients with indwelling recording electrodes," Electroenceph. Clin. Neurophysiol., vol. 86, pp. 428-437, 1993.

[16] A. M. Murro, Don W. King et al., "Computerized seizure detection of complex partial seizure," Electroenceph. Clin. Neurophysiol., vol. 79, pp. 330-333, 1991.

[17] W. R. S. Webber, Ronald P. Lesswer et al., "An approach to seizure detection using an artificial neural network (ANN)," Electroenceph. Clin. Neurophysiol., vol. 98, pp. 250-272, 1996.

[18] A. J. Gabor, "Automated seizure detection using a self-organizing neural network: validation and comparison with other strategies," Electroenceph. Clin. Neurophysiol., vol. 99, pp. 257-266, 1996.

[19] A. J. Gabor, "Seizure detection using a self-organizing neural network: validation and comparison with other strategies," Electroenceph. Clin. Neurophysiol., vol. 107, pp. 27-32, 1998.

[20] Bergey GK, Franaszczuk PJ., "Epileptic seizures are characterized by changing signal complexity," Clinical Neurophysiology, vol. 112, no. 2, pp. 241-249, 2001.

[21] L. Diambra, J. C. Bastos et al., "Epileptic activity recognition in EEG recording," Physica A, vol. 273, pp. 495-505, 1999.

[22] J. Gotman, "Practical use of computer-assisted EEG interpretation in epilepsy, Journal of Clinical Neurophysiology," vol. 2, no. 3, pp. 251-265, 1985.

[23] R. Agarwal, "Enhancement –techniques of short-duration narrowband signals with application to ABR audiometry," 1995, Ph. D. thesis, Concordia University.

[24] R. Agarwal, E. I. Plotkin, and M. N. S. Swamy, "Statistically optimal null filter based on instantaneous matched processing," Circuits Systems and Signal Processing, vol. 20, no. 1, pp. 37-61, 2001.

[25] Liying Shi, Rajeev Agarwal, and M.N.S. Swamy, "Model-Based Seizure Detection Method using Statistically Optimal Null Filters," EMBS conference paper 1.1.2-5, pp 161, 2004, San Francisco.

[26] V. Fransisco, et al., "A Study on the Best Order of AR EEG Modeling," Int. J. Biomedical Computing, vol. 20, pp. 41-50, 1987.

[27] F. Yang and S. Gao, Biomedical Signal Processing, High-Education Press, 1989, Beijing,China.

[28] P. Celka, and P. Colditz, "A computer-aided detection of EEG seizures in infants: A singular-spectrum approach and performance comparison," IEEE Trans. Biomed. Eng., vol. 49, no. 5, pp. 455-462, 2002.

[29] J. Gotman, D. Flanagan, J. Zhang, and B. Rosenblatt, "Evaluation of an automatic seizure detection method for the newborn EEG," Electroenceph. Clin. Neurophysiol., vol. 103, pp. 363-369, 1997.

Appendix

Investigation of SONF via simulation

This appendix is intended to explain why the high-amplitude artifact at the start of some of the EEG segments may cause false detections. For this purpose, we consider the following two cases.

Case 1. Input x=10.0*sin(2*pi* ω_0 *k), 0< k ≤ 1200

Basis functions: bf1= sin(2*pi* ω_0 *k); bf2=cos(2*pi* ω_0 *k);

Figure A.1 shows the input and output of the SONF (ideal case, output tracks input exactly). Figure A.2 shows the λ and υ distributions, where $\lambda's$ are the scaling functions in the SONF, and $\upsilon's$ are the outputs of the IMF in the SONF. More detail can be found in Chapter 2.

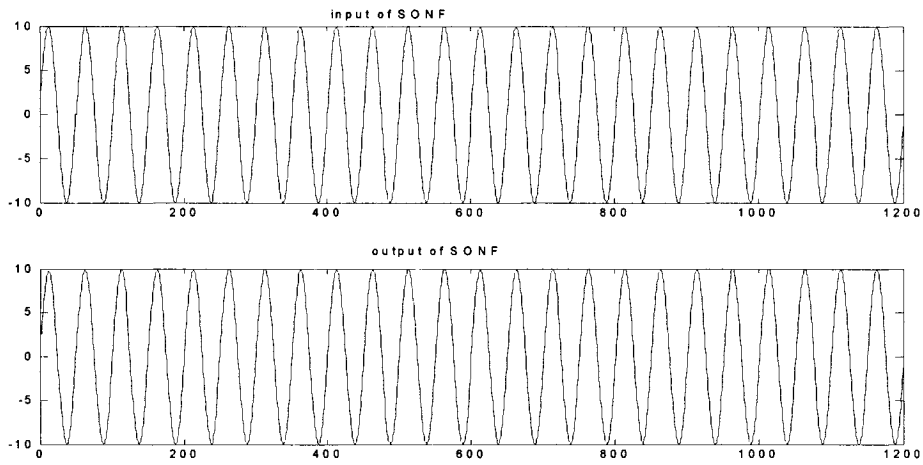

Figure A.1 Input and output of SONF

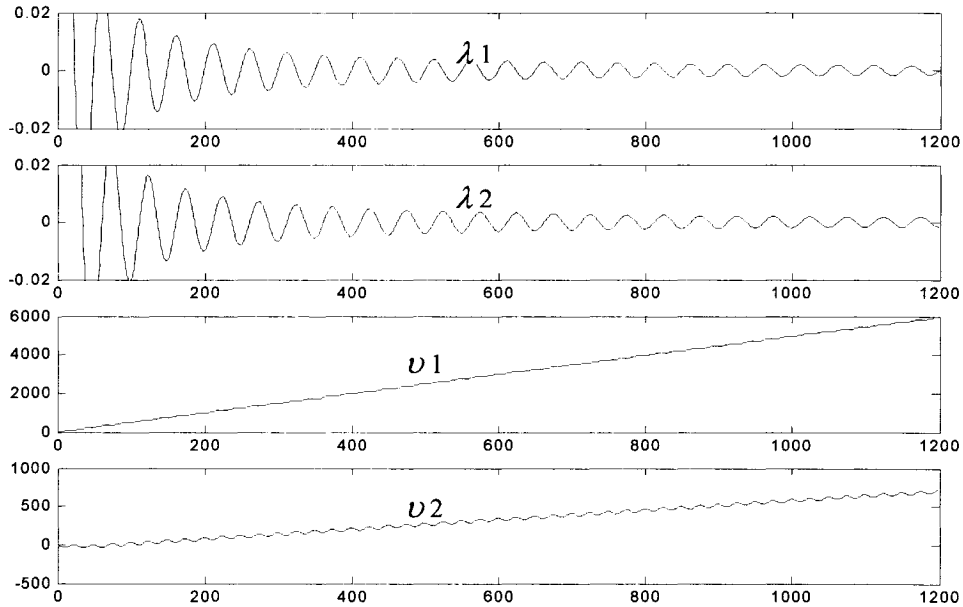

Figure A.2 λ and υ ($\lambda 1$ and $\lambda 2$, $\upsilon 1$ and $\upsilon 2$ represent the two branches of SONF)

Case 2. Input $x=\begin{cases} 10*\sin(2*pi*\omega_0*k) & 0<k<50 \\ \sin(2*pi*\omega_1*(k-50)), & 50\le k\le 1200 \end{cases}$

Basis functions: bf1= sin (2*pi* ω_0 *k); bf2=cos (2*pi* ω_0 *k);

Figure A.3 shows the input and output of the SONF (output cannot track the input properly). Figure A.4 shows the λ and υ distributions.

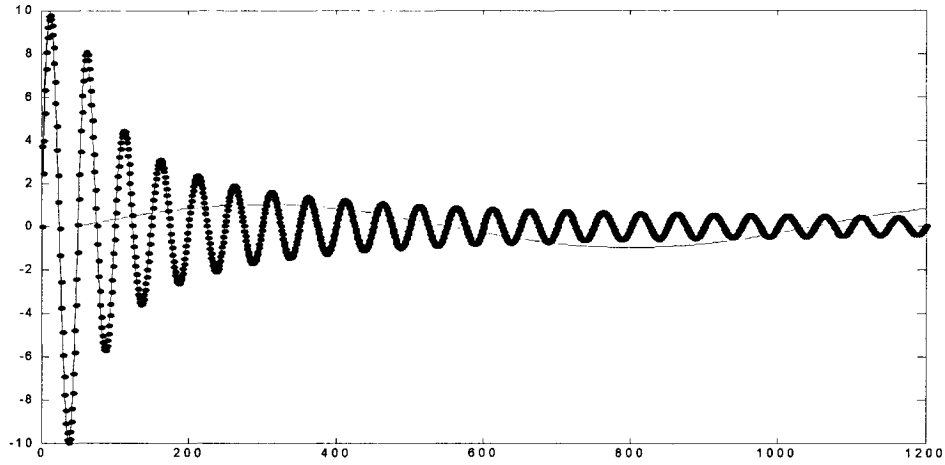

Figure A.3 Input and output of SONF. Solid line: input. Dotted line: output.

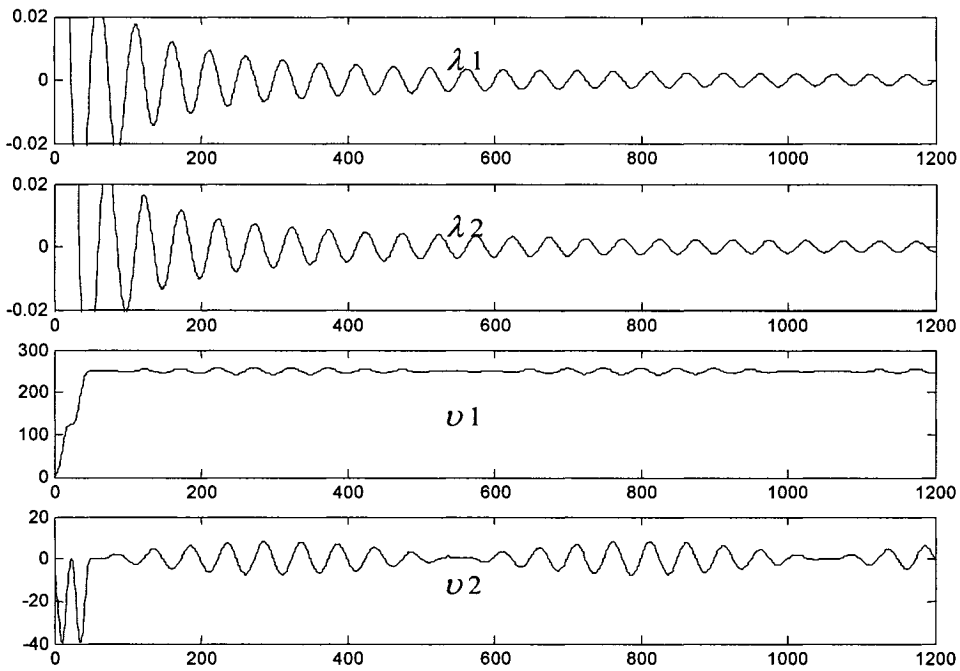

Figure A.4 λ and υ ($\lambda 1$ and $\lambda 2$, $\upsilon 1$ and $\upsilon 2$ represent the two branches of SONF)

Figures A.3 and A.4 show that the output can't track the input properly when there is a high-amplitude artifact at the start of the data segment. For the first 50 samples, the output tracks the input very well. But after the first 50 samples, even though the input signal does not have ω_0 frequency component, SONF still gives the output with frequency ω_0. The energy ratio of the output and input at this situation will be large, making it possible for a false detection to occur.

Refer to the recursive algorithm of the globally optimal SONF in Chapter 2. The gain matrix P(n) is only related to the basis functions ϕ(n). Hence, when ϕ(n) is fixed, P(n) and λ(n) are fixed.

The output $\upsilon(n)$ of the *instantaneous matched filter* (IMF) is calculated using the recursive equation $\upsilon(n) = \upsilon(n-1) + x(n)\phi(n)$, and the initial value $\upsilon(0) = x(0)\phi(0)$.

The output of the SONF is $y'(n) = \lambda^T(n)\upsilon(n)$

The equation can be extended as

$$y'(n) = \lambda^T(n)\upsilon(n) = \lambda^T(n)[x(n)\phi(n) + x(n-1)\phi(n-1) + ... + x(0)\phi(0)]$$

Hence, the output at sample *n* relies on the input samples from 0 *to* *n*-1. This can explain the phenomena in Figure A.3.